THE JOURNAL OF BIOLOGICAL CHEMISTRY VOL. 287, NO. 48, pp. 40441–40447, November 23, 2012

Leptin Activates Hepatic 5′-AMP-activated Protein Kinase through Sympathetic Nervous System and α1-Adrenergic Receptor

*A POTENTIAL MECHANISM FOR IMPROVEMENT OF FATTY LIVER IN LIPODYSTROPHY BY LEPTIN**

Received for publication, June 16, 2012, and in revised form, September 24, 2012 Published, JBC Papers in Press, September 28, 2012, DOI 10.1074/jbc.M112.384545

Licht Miyamoto[‡1], Ken Ebihara[‡§2], Toru Kusakabe[‡], Daisuke Aotani[‡], Sachiko Yamamoto-Kataoka[‡], Takeru Sakai[‡], Megumi Aizawa-Abe[‡§], Yuji Yamamoto[‡], Junji Fujikura[‡], Tatsuya Hayashi[¶], Kiminori Hosoda[‡§‖], and Kazuwa Nakao[‡§]

From the [‡]Department of Medicine and Clinical Science, Kyoto University Graduate School of Medicine and the [§]Translational Research Center, Kyoto University Hospital, 54 Shogoin Kawahara-cho, Sakyo-ku, Kyoto 606-8507, the [¶]Kyoto University Graduate School of Human and Environmental Studies, Yoshida-Nihonmatsu-cho, Sakyo-ku, Kyoto 606-8501, and the [‖]Department of Human Health Science, Kyoto University Graduate School of Medicine, 54 Shogoin Kawahara-cho, Sakyo-ku, Kyoto 606-8507, Japan

Background: AMPK activation promotes glucose and lipid metabolism.
Results: Hepatic AMPK activities were decreased in fatty liver from lipodystrophic mice, and leptin activated the hepatic AMPK via the α-adrenergic effect.
Conclusion: Leptin improved the fatty liver possibly by activating hepatic AMPK through the central and sympathetic nervous systems.
Significance: Hepatic AMPK plays significant roles in the pathophysiology of lipodystrophy and metabolic action of leptin.

Leptin is an adipocyte-derived hormone that regulates energy homeostasis. Leptin treatment strikingly ameliorates metabolic disorders of lipodystrophy, which exhibits ectopic fat accumulation and severe insulin-resistant diabetes due to a paucity of adipose tissue. Although leptin is shown to activate 5′-AMP-activated protein kinase (AMPK) in the skeletal muscle, the effect of leptin in the liver is still unclear. We investigated the effect of leptin on hepatic AMPK and its pathophysiological relevance in A-ZIP/F-1 mice, a model of generalized lipodystrophy. Here, we demonstrated that leptin activates hepatic AMPK through the central nervous system and α-adrenergic sympathetic nerves. AMPK activities were decreased in the fatty liver of A-ZIP/F-1 mice, and leptin administration increased AMPK activities in the liver as well as in skeletal muscle with significant reduction in triglyceride content. Activation of hepatic AMPK with A769662 also led to a decrease in hepatic triglyceride content and blood glucose levels in A-ZIP/F-1 mice. These results indicate that the down-regulation of hepatic AMPK activities plays a pathophysiological role in the metabolic disturbances of lipodystrophy, and the hepatic AMPK activation is involved in the therapeutic effects of leptin.

Leptin is an adipocyte-derived hormone that regulates energy homeostasis mainly through the hypothalamus (1, 2). In addition to food intake and energy expenditure, leptin regulates glucose and lipid metabolism. Indeed, the usefulness of leptin treatment in various types of diabetes, including type 1, type 2, and lipoatrophic diabetes, has been demonstrated in rodent models (3–8). The clinical application of leptin treatment has already begun (9–12), especially in lipoatrophic diabetes that develops with lipodystrophy.

Lipodystrophy is a disease characterized by a paucity of adipose tissue that leads to leptin deficiency. Patients with lipodystrophy generally suffer severe insulin-resistant diabetes. Although the molecular mechanism by which insulin resistance develops in lipodystrophy is not fully understood, ectopic fat accumulation in insulin target tissues such as skeletal muscle and liver is thought to be one of the major causes for insulin resistance. The pathological condition in which ectopically accumulated fat exerts adverse effects against the cellular function is referred to as "lipotoxicity" (13). The amount of fat accumulated in tissues is known to correlate with the severity of insulin resistance (14). Lipoatrophic patients frequently develop severe fatty liver and excess fat accumulation in the skeletal muscle (15).

We and others have demonstrated that leptin effectively improves insulin sensitivity accompanied by dramatic reduction of fat content in the liver and skeletal muscle in patients

* This work was supported in part by research grants from the Ministry of Education, Culture, Sports, Science and Technology of Japan, the Ministry of Health, Labor and Welfare of Japan, The Takeda Medical Research Foundation, The Japan Foundation of Applied Enzymology, Eli Lilly and Co., and The Nakatomi Foundation.
[1] Present address: Dept. of Medical Pharmacology, Institute of Health Biosciences, University of Tokushima Graduate School, 1-78-1 Shou-machi, Tokushima-shi, Tokushima 770-8505, Japan.
[2] To whom correspondence should be addressed: 54 Shogoin Kawahara-cho, Sakyo-ku, Kyoto 606-8507, Japan. Tel.: 81-757513173; Fax: 81-757719452; E-mail: kebihara@kuhp.kyoto-u.ac.jp.

with lipodystrophy (3, 9–12). Using rodent models, it was demonstrated that leptin activates AMPK[3] in the skeletal muscle through both central and direct pathways (16). AMPK is a heterotrimeric enzyme that is conserved from yeast to humans and functions as a "fuel gauge" to monitor the status of cellular energy. AMPK potently stimulates fatty acid oxidation by inhibiting the activity of acetyl-CoA carboxylase (17). Thus, AMPK activation by leptin is a plausible mechanism by which leptin reduces ectopic fat in the skeletal muscle.

In addition to the skeletal muscle, recent studies have shown the physiological significance of AMPK in the liver (18–20). However, the effect of leptin on hepatic AMPK activity remains to be determined. The role of AMPK in the pathogenesis of metabolic abnormalities in lipodystrophy also remains unclear. In this study, we investigated the effect of leptin on hepatic AMPK activities and the pathophysiological role of AMPK in A-ZIP/F-1 mice, a well established mouse model of generalized lipodystrophy (21).

EXPERIMENTAL PROCEDURES

Materials and Animals—All reagents were analytic grade and obtained from Sigma unless otherwise stated. C57BL/6J mice and Wistar rats were purchased from Japan SLC, Inc. The F1 mice analyzed in Fig. 4 were obtained by crossing male A-ZIP/F-1 mice on the FVB/N background with female leptin transgenic mice on the C57BL/6J background (3, 22). A-ZIP/F-1 and the F1 mice were studied with appropriate littermate controls. Mice and rats were housed in an animal facility maintained at 20 °C with a 12:12-h light/dark cycle, allowed free access to water and standard rodent chow, and were randomly assigned to experimental groups. The mice were analyzed at the age of 9–10 weeks (C57BL/6J) or 15 weeks (A-ZIP/F-1, F1). Kyoto University Graduate School of Medicine Committee on Animal Research approved all experimental procedures.

Drug Administration—For continuous treatment, leptin was administered for 6 days using a subcutaneously implanted osmotic pump (Durect) at the dose of 0.65 mg/kg/day. For single intraperitoneal and intracerebroventricular (i.c.v.) injection, the dose of leptin was 1 mg/kg and 1 μg/mouse, respectively. Prazosin (2.5 mg/kg/day) or propranolol (1 mg/kg/day) was continuously co-administered with leptin for 6 days using an independently implanted osmotic pump. A769662 was administered once daily by intraperitoneal injection at the dose of 30 mg/kg/day for 4 days.

Primary Hepatocyte—Hepatocytes were isolated from male Wistar rats (100–150 g) by a two-step collagenase perfusion. The portal vein was cannulated under chloral hydrate anesthesia, and the liver was perfused with hepatocyte liver perfusion medium and digest medium (Invitrogen). After perfusion, hepatocytes were purified by filtration (100-μm mesh) and centrifuged (100 × *g*, 1 min, four times) and seeded onto 6-well culture plates coated with type I collagen (Iwaki) (1×10^6 cells/well). Cells were cultured in DMEM containing 10% FBS, 100 nM insulin, 100 nM dexamethasone, 30 mg/liter kanamycin, and 5 units/ml aprotinin for 12 h, and the medium were replaced with DMEM containing 10% FBS, 1 nM insulin, 1 nM dexamethasone, 30 mg/liter kanamycin, and 5 units/ml aprotinin for 6 h prior to stimulation. The cells were stimulated by 100 ng/ml leptin, 1 mM 5-aminoimidazole-4-carboxamide 1-β-D-ribofuranoside or 0.5 mM 2,4-dinitrophenol for the indicated times.

Hepatic Vagotomy—Hepatic vagotomy was performed as described previously (23, 24) with modifications. Briefly, a hepatic branch of the ventral subdiaphragmatic vagal trunk was cleft using micro scissors under ether anesthesia, and the abdominal muscle wall and skin incision was closed with silk sutures. Drugs were introduced 1 week after the surgery. Accomplishment of the amputation was visually confirmed when sampling.

Chemical Sympathectomy—C57BL/6J mice were chemically sympathectomized by continuous infusion of guanethidine (30 mg/kg/day) for 6 days as described above.

Tissue Sampling and Biochemical Analysis—Tissues were rapidly isolated and frozen in liquid nitrogen by freeze-clamping (25) under chloral hydrate anesthesia after starvation for 6 h. Mice had been starved for 4 h previous to and during the study in a single administration study. Blood glucose was determined by reflectance glucometer under *ad libitum* feeding conditions. Plasma leptin was measured by RIA (Linco). Plasma insulin (Morinaga), adiponectin (Linco), and interleukin-6 (R&D Systems) were measured by ELISA. Triglyceride content was determined by E-test kit (Wako) in 2-propanol/heptane extract of the tissues. Homeostasis model assessment insulin resistance (HOMA-IR) was calculated on the assumption that the titer of murine insulin is as much as that of human insulin.

Isoform-specific AMPK Activity—AMPK activities were determined as described previously (26). Briefly, frozen tissues were homogenized in Hepes/Triton-based lysis buffer and then centrifuged. The supernatants were immunoprecipitated with protein A-Sepharose beads and isoform-specific antibodies against AMPK α1 or α2 (Millipore). Kinase activities in the immune complex were determined by the phosphorylation of the SAMS peptide using [γ-^{32}P]ATP.

Western Blotting Analysis—40 μg of protein per each sample was subjected to SDS-PAGE using 4–12% BisTris gel (Bio-Rad). Antibodies were from Cell Signaling Technology or Merck. ECL Plus (GE Healthcare) and LAS-1000 image analyzer (Fuji film) were used for detection and quantification.

Quantitative Analysis of Gene Expressions—Total RNA was prepared using Isogen (Molecular Research Center). mRNA levels were quantified by real time PCR with the Taqman method (ABI Prism 7300). Primer sets and probes were as follows: 18 S, CGCGCAAATTACCCACTCCCGA, CGGCTACCACATCCAAGGA, and CCAATTACAGGGCCTCGAAA; AMPKα1, TGCAAAGATAGCCGACTTTGGTCTTTCA, GAACGTCCTGCTTGATGCACACAT, and TGGGTGAGCCACAGCTTGTTCTTA; and AMPKα2, TGATTCCAGCACAGCTGAGAACCACT, AAGCATCGATGATGAGGTGGTGGA, and ACAAAGTGCTGCCAGTCAAAGAGC (probe, forward, and reverse, respectively) Relative amounts of mRNAs were normalized with the ribosomal 18 S RNA.

[3] The abbreviations used are: AMPK, 5′-AMP-activated protein kinase; A-ZIP, A-ZIP/F-1 mice; LepTg, transgenic mice overexpressing leptin; BisTris, 2-[bis(2-hydroxyethyl)amino]-2-(hydroxymethyl)propane-1,3-diol; HOMA-IR, homeostasis model assessment insulin resistance; i.c.v., intracerebroventricular.

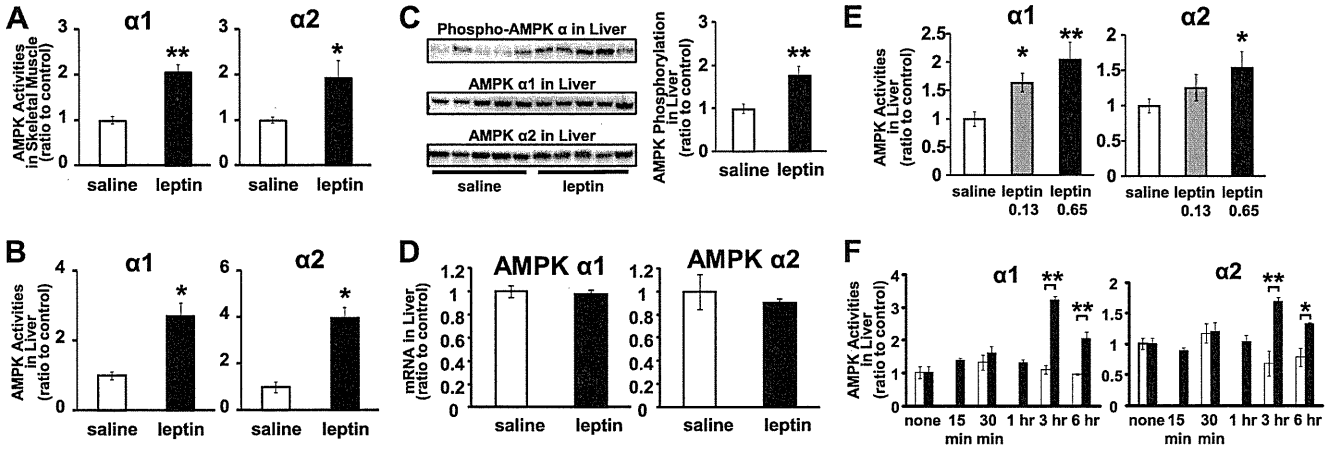

FIGURE 1. **AMPK activation in skeletal muscle and liver by leptin administration.** Isoform-specific AMPK activities in gastrocnemius muscle (*A*) and liver (*B*) from C57BL/6J mice after continuous saline or leptin administration are shown. Western blot analyses for phospho-AMPKα, AMPK α1 and α2 (*C*), and AMPK α1 and α2 mRNA levels normalized to 18 S ribosomal RNA (*D*) in liver are shown. AMPK activities in liver after 0.13 and 0.65 mg/kg/day continuous leptin infusion (*E*) are shown. AMPK activities in liver 15 min to 6 h after single intraperitoneal injection of saline or leptin (*F*) are shown. Data are shown as ratios to saline or quiescent control (mean ± S.E.). □, saline; ■, leptin. $n = 4-6$. *, $p < 0.05$; **, $p < 0.01$ *versus* saline.

Statistical Analyses—Two groups were compared by Student's *t* test. Comparisons between multiple groups were evaluated by analysis of variance. $p < 0.05$ was considered statistically significant.

RESULTS

Effect of Leptin Treatment on AMPK α1 and α2 Activities in Skeletal Muscle and Liver—The isoform-specific AMPK activities in skeletal muscles and liver were determined in leptin- and saline-treated mice. Both AMPK α1 and α2 activities in skeletal muscle were increased 2-fold in leptin-treated mice compared with saline-treated mice (Fig. 1*A*). AMPK α1 and α2 activities in the liver were also increased 2.5- and 3.5-fold, respectively (Fig. 1*B*). The phosphorylation of AMPK α was also increased in leptin-treated mice compared with saline-treated mice (Fig. 1*C*). Meanwhile, protein or mRNA expressions of AMPK α1 and α2 in the liver were not significantly different between leptin- and saline-treated mice (Fig. 1, *C* and *D*). Therefore, the increase of AMPK activities in the liver from leptin-treated mice was not due to the increase in their expression levels.

When leptin was administered continuously, the activation of AMPK in the liver was dose-dependent (Fig. 1*E*). After intraperitoneal single leptin injection, the activation of both AMPK α1 and α2 was detected from 3 h while no activation was observed within 1 h (Fig. 1*F*).

Mechanism of Hepatic AMPK Activation by Leptin—To clarify whether leptin acts directly on hepatocytes, we examined AMPK activities in isolated primary rat hepatocytes with or without leptin (Fig. 2*A*). The addition of leptin into the culture medium increased neither AMPK α1 nor α2 activities. Next, we examined the effect of leptin i.c.v. injection on AMPK activities in the liver (Fig. 2*B*). The activation of both AMPK α1 and α2 was detected 3 h after leptin injection at the dose that did not cause any effect when administered peripherally. These results indicate that leptin activates AMPK in the liver mainly through the CNS.

Therefore, we examined the involvement of autonomic nerves in the effect of leptin on AMPK activation in the liver. Hepatic vagotomy did not show any effect on AMPK activation by leptin in the liver (Fig. 2*C*). In contrast, chemical sympathectomy by guanethidine treatment completely inhibited the activation of both AMPK α1 and α2 by leptin in the liver (Fig. 2*D*). We further investigated the involvement of the subtype-specific sympathetic nervous system. Administration of propranolol, a β-antagonist, did not suppress AMPK activation in the liver, whereas prazosin, an α1-antagonist, completely inhibited the activation of both AMPK α1 and α2 by leptin in the liver (Fig. 2, *E* and *F*).

AMPK α1 and α2 Activities in Skeletal Muscle and Liver from A-ZIP/F-1 Mice—To explore the pathophysiological role of AMPK in lipodystrophy, we examined AMPK α1 and α2 activities in skeletal muscle and liver from A-ZIP/F-1 (A-ZIP) mice. Characteristics of A-ZIP mice used in this study are shown in Table 1. Consistent with previous studies (21), A-ZIP mice showed hyperglycemia and hyperinsulinemia, suggesting insulin resistance, and also showed increased liver weight, suggesting fatty liver. Plasma leptin and adiponectin levels were markedly decreased, but the plasma interleukin-6 level was not significantly different from that in WT mice. In these A-ZIP mice, both AMPK α1 and α2 activities in the liver were apparently decreased compared with WT mice, although those in the skeletal muscle were not significantly different from WT mice (Fig. 3, *A* and *B*). AMPK α1 and α2 mRNA expressions in the skeletal muscle were not significantly different in A-ZIP mice, and those in the liver were rather increased compared with WT mice (Fig. 3, *C* and *D*). Therefore, the decrease in AMPK activities in the liver from A-ZIP mice was not due to the change in their mRNA expressions. However, leptin treatment effectively increased AMPK α1 and α2 activities in the liver as well as in the skeletal muscle from A-ZIP mice (Fig. 3, *E* and *F*).

Effect of Transgenic Overexpression of Leptin on AMPK α1 and α2 Activities in Skeletal Muscle and Liver from A-ZIP/F-1 Mice—To explore the chronic effect of leptin, we crossed transgenic mice overexpressing leptin (LepTg) and A-ZIP mice, producing mice of four genotypes as follows: WT, LepTg, A-ZIP, and A-ZIP/LepTg. AMPK α1 and α2 activities in both the skel-

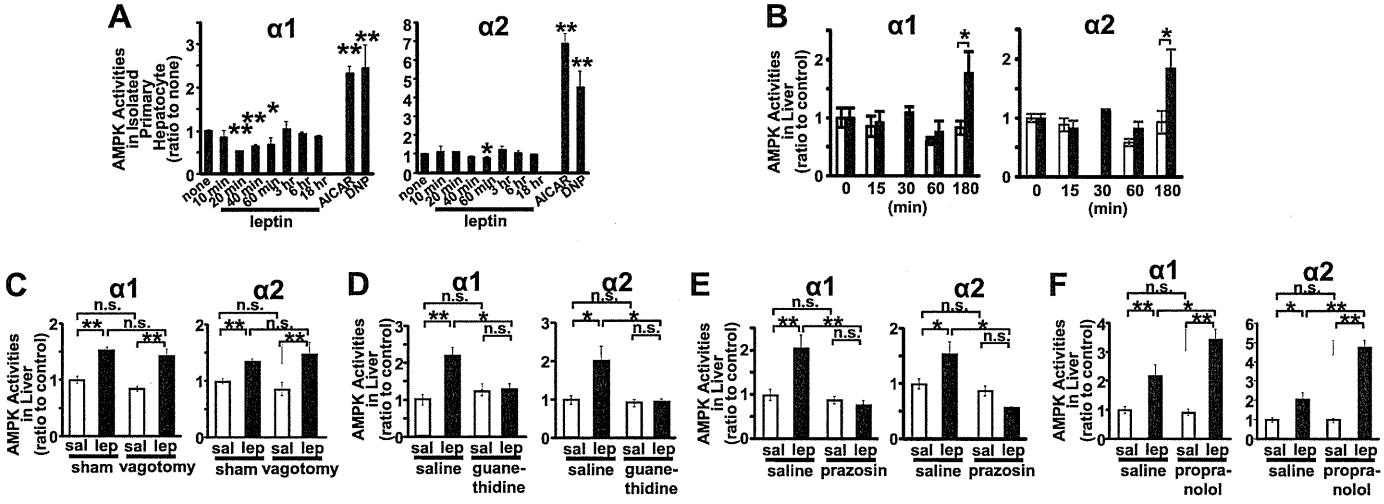

FIGURE 2. **Mechanism of hepatic AMPK activation by leptin administration.** AMPK activities in isolated rat primary hepatocytes 10 min to 18 h after stimulation by leptin, 5-aminoimidazole-4-carboxamide 1-β-D-ribofuranoside (*AICAR*) (40 min), or 2,4-dinitrophenol (*DNP*) (15 min) (*A*) are shown. AMPK activities in liver 15 min to 3 h after i.c.v. administration of saline (*sal*) or leptin (*lep*) (*B*). The effects of hepatic vagotomy (*C*), chemical sympathectomy (*D*), co-administration of antagonists against α1-adrenoreceptors (*E*) or β-adrenoreceptors (*F*) on hepatic AMPK activation by leptin are shown. Data are shown as ratios to saline or quiescent control (mean ± S.E.). $n = 4–6$ (*A*, and *C–E*); $n = 3–6$ (*B*). *, $p < 0.05$; **, $p < 0.01$ *versus* control. *n.s.*, not significant.

TABLE 1

Characteristics of A-ZIP/F-1 mice used in this study

Values are as follows: $n = 8–11$ (glucose); $n = 3–5$ (leptin); $n = 5–7$ (other adipocytokines).

	WT	A-ZIP/F-1 mice
Body weight	30.7 ± 0.8 g	32.5 ± 0.4 g
Glucose	167 ± 5.8 mg/dl	331 ± 39 mg/dl[a]
Insulin	0.24 ± 0.0 ng/ml	0.46 ± 0.1 ng/ml[b]
Leptin	6.15 ± 1.3 ng/ml	1.25 ± 0.5 ng/ml[b]
Adiponectin	6.27 ± 0.4 μg/ml	1.46 ± 0.5 μg/ml[a]
Interleukin-6	5.3 ± 0.8 pg/ml	6.5 ± 1.0 pg/ml
Liver weight	1.19 ± 0.0 g	1.98 ± 0.2 g[a]

[a] $p < 0.01$ *versus* WT. Data are expressed as means ±S.E.
[b] $p < 0.05$ *versus* WT. Data are expressed as means ±S.E.

etal muscle and liver were markedly increased in LepTg mice (Fig. 4, *A* and *B*). At this time, triglyceride contents in skeletal muscle and liver in LepTg mice were reduced to more than half of those in WT mice (Fig. 4, *C* and *D*). AMPK activities were unchanged in the skeletal muscle but were apparently decreased in the liver from A-ZIP mice when compared with WT mice (Fig. 4, *A* and *B*). As to triglyceride contents, the apparent increment was observed in both the skeletal muscle and liver in A-ZIP mice (Fig. 4, *C* and *D*). However, AMPK activities were increased, and triglyceride content was decreased in A-ZIP/LepTg mice as well as in LepTg mice in both the skeletal muscle and liver (Fig. 4, *A–D*). In accordance with our previous report, blood glucose and plasma insulin levels were lower in LepTg mice than in WT mice, and severe hyperglycemia and hyperinsulinemia in A-ZIP mice were strikingly ameliorated by transgenic overexpression of leptin (Fig. 4, *E* and *F*) (3).

Effect of AMPK Activator, A769662, on AMPK Activities and Triglyceride Content in Skeletal Muscle and Liver from A-ZIP/F-1 Mice—After intraperitoneal single injection of A769662, an AMPK-specific activator, the activity of AMPK α1 was increased but that of α2 was not significantly increased in the skeletal muscle (Fig. 5*A*). The activity of both AMPK α1 and α2 was clearly increased in the liver (Fig. 5*B*). Although repetitive injection of A769662 for 4 days did not signifi-

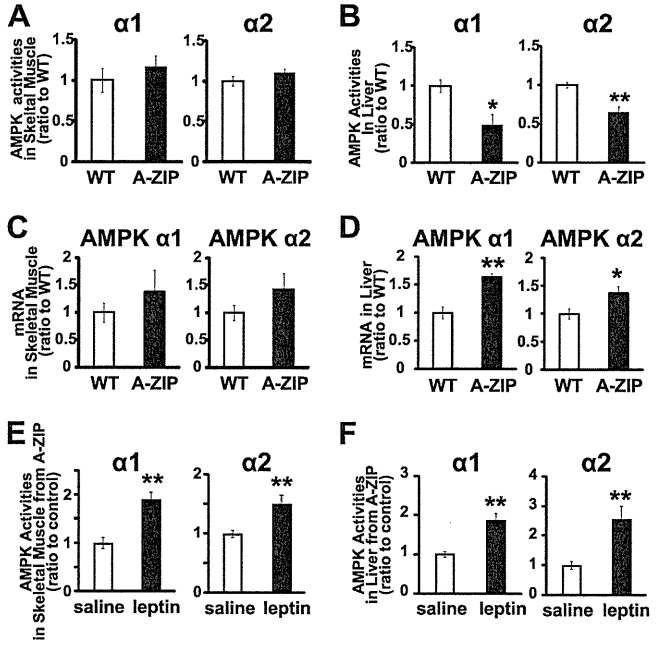

FIGURE 3. **AMPK activities and mRNA expressions in a mouse model of lipoatrophic diabetes.** α1- and α2-isoform-specific AMPK activities in the soleus muscle (*A*) and liver (*B*) are shown. AMPK α1 and α2 mRNA levels in the soleus muscle (*C*) and liver (*D*) normalized to 18 S ribosomal RNA are shown. AMPK activities in gastrocnemius muscle (*E*) and liver (*F*) from A-ZIP/F-1 mice after continuous leptin administration are shown. Data are shown as ratios to WT or saline control (mean ± S.E.). □, WT; ■, A-ZIP/F-1. $n = 4–5$. (*A–D*). □, saline; ■, leptin. $n = 9–10$ (*E* and *F*). *, $p < 0.05$; **, $p < 0.01$ *versus* control.

cantly reduce triglyceride content in the skeletal muscle, it effectively reduced triglyceride content to one-third of that in saline-treated mice in the liver (Fig. 5, *C* and *D*). At this time, the blood glucose level was significantly decreased, and HOMA-IR, an index of insulin resistance, tended to be decreased although plasma insulin level was not significantly decreased (Fig. 5, *E–G*). Food intake and body weight were not affected by A769662 (Fig. 5, *H* and *I*).

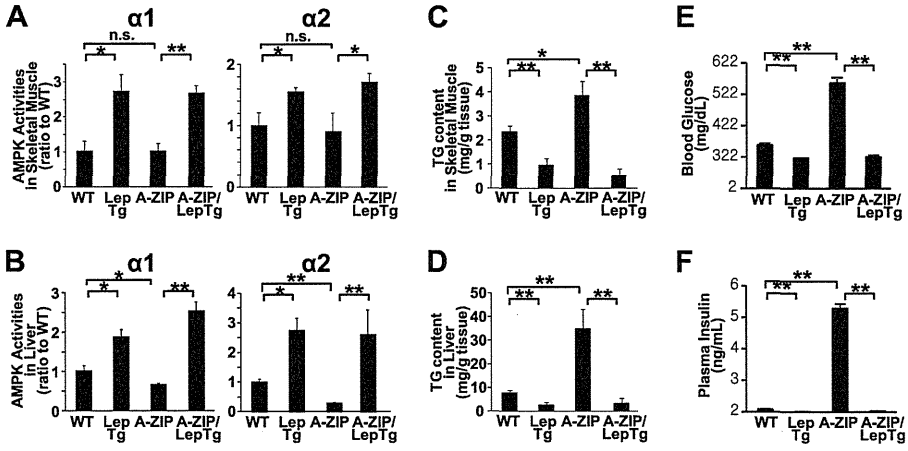

FIGURE 4. **AMPK activation and reduction in ectopic triglyceride accumulation in skeletal muscle and liver from leptin transgenic mice and double transgenic A-ZIP/LepTg mice.** AMPK activities in gastrocnemius muscle (*A*) and liver (*B*), triglyceride content in gastrocnemius muscle (*C*) and liver (*D*), and blood glucose levels (*E*) and plasma insulin levels (*F*) from F1 mice obtained by crossing A-ZIP/F-1 mice and leptin transgenic mice are shown. Data are shown as ratios to +/+ (mean ± S.E.). $n = 4–7$. *, $p < 0.05$; **, $p < 0.01$; *n.s.*, not significant.

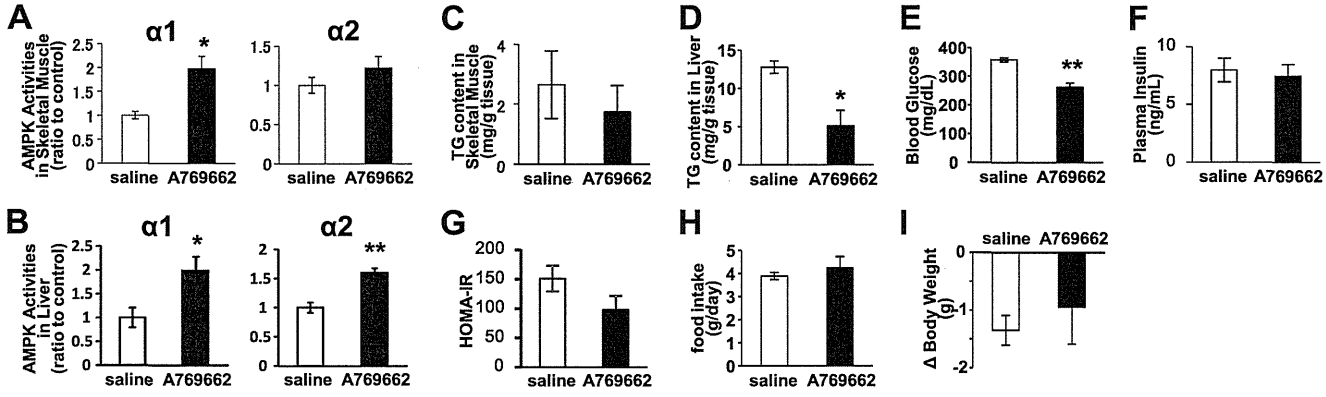

FIGURE 5. **Resolution of fatty liver in A-ZIP/F-1 mice by AMPK activation.** AMPK activities in gastrocnemius muscle (*A*) and liver (*B*) 30 min after a single intraperitoneal injection of AMPK activator, A769662 (30 mg/kg) are shown. Triglyceride contents in gastrocnemius muscle (*C*) and liver (*D*), blood glucose (*E*), plasma insulin (*F*), and calculated HOMA-IR (*G*) after the repetitive A769662 administration (30 mg/kg/day for 4 days) are shown. Food intake (*H*) and weight change (*I*) during the study period are shown.

DISCUSSION

This is the first report clearly demonstrating that leptin activates hepatic AMPK through the central nervous system and an α-adrenergic effect *in vivo*. It had long been unclear whether leptin activates hepatic AMPK *in vivo*. It was reported that adenovirus-induced leptin overexpression failed to increase hepatic AMPK activities (27). However, leptin-induced suppression of gluconeogenesis was abolished in liver-specific AMPK α2 knock-out mice, suggesting that leptin suppresses gluconeogenesis through hepatic AMPK activation (18). Furthermore, a slight increase in hepatic AMPK activity 45 min after leptin administration was reported in mice, although it has been deemed as an artificial effect (28, 29). In this study, we demonstrated that hepatic AMPK activation by leptin is dose-dependent (Fig. 1*E*), and hepatic AMPK activity clearly increases from 3 h after leptin administration in mice (Fig. 1*F*).

In the skeletal muscle, AMPK is reported to be activated by leptin both directly on skeletal muscles and indirectly through the hypothalamic relay (16). In the liver, this study demonstrated that leptin activates AMPK mainly through the CNS and that leptin has no direct AMPK-activating effect on hepatocytes (Fig. 2, *A* and *B*). There is a report showing the increase in AMPK phosphorylation by leptin using Huh7 human hepatoma cells overexpressing leptin receptors; however, it was observed only in the receptor-overexpressing cells (30). AMPK activation in the skeletal muscle by leptin is biphasic, and the former phase, which occurred in 15 min, is caused by direct muscle stimulation (16). Meanwhile, hepatic AMPK activation was detected only from 3 h after leptin administration, supporting the notion that leptin activates hepatic AMPK mainly through the CNS.

The parasympathetic and sympathetic nervous systems between the hypothalamus and liver play an important role in regulating metabolism (31). In this study, chemical sympathectomy completely inhibited hepatic AMPK activation by leptin although hepatic vagotomy did not, indicating that leptin activates hepatic AMPK mainly through the sympathetic nervous system (Fig. 2, *C* and *D*). Moreover, we demonstrated that hepatic AMPK activation by leptin was mainly dependent on the α-adrenergic effect but not on the β-adrenergic effect (Fig. 2, *E* and *F*). Not the β- but the α1-adrenoreceptor stimulation was shown to activate AMPK in isolated skeletal muscle, L6 myotubes, H9C2 cardiomyocyte, and rat heart (16, 32, 33), although not the α1- but the β-adrenoreceptors mediate AMPK activation in brown and white adipocytes (32, 34). The

physiological significance of this adrenoreceptor tissue specificity will be an issue in the future.

Recent reports have revealed some adipocytokines harbor the potential to activate AMPK in the liver or skeletal muscle. AMPK potently stimulates fatty acid oxidation by inhibiting the activity of acetyl-CoA carboxylase (17). Thus, we hypothesized that AMPK might play a pathophysiological role in ectopic fat accumulation and marked insulin resistance developed in lipodystrophy. Indeed, analysis of A-ZIP mice revealed the decrease in AMPK activities in the liver, suggesting the pathophysiological significance of hepatic AMPK in the development of fatty liver in lipodystrophy (Fig. 3*B*).

It is interesting that AMPK activities in the skeletal muscle were not decreased in A-ZIP mice when compared with WT mice. Basal AMPK activities in the skeletal muscle in *fa/fa* rats were also not different from those from control rats (35, 36), although AMPK activities in the liver in *fa/fa* rats and *ob/ob* mice were decreased (37). Although it is unknown what determines the difference between the skeletal muscle and the liver, some factors may counteract the decrease of AMPK activities brought by leptin deficiency in the skeletal muscle.

We previously showed that transgenic overexpression of leptin strikingly improves metabolic abnormalities in A-ZIP mice (3). Insulin-stimulated PI3K activity in the skeletal muscle and liver were amplified in LepTg mice (22). However, the underlying molecular mechanisms of metabolic action of leptin have not been fully clarified. Although leptin was reported to activate AMPK in the skeletal muscle (16), the effect of leptin on hepatic AMPK activity had been unclear. We found that leptin activates both isoforms of AMPK not only in the skeletal muscle but also in the liver in association with the reduction of tissue triglyceride content in A-ZIP mice (Fig. 4). These results indicated the therapeutic role of AMPK in the metabolic improvement by leptin in lipodystrophy.

To confirm the therapeutic role of hepatic AMPK in the improvement of fatty liver by leptin in lipodystrophy, we investigated the effect of A769662, an AMPK-specific activator on liver triglyceride content in A-ZIP mice. A769662 was shown to activate AMPK and decrease acetyl-CoA carboxylase activity and triglyceride in the liver of *ob/ob* mice (38). It was also reported that A769662 preferably works on the liver *in vivo* due to the preference of tissue distribution of A769662 after injection (38). Indeed, although A769662 significantly activated only AMPK α1 and did not significantly decrease triglyceride content in the skeletal muscle, it effectively activated both AMPK α1 and α2 and reduced triglyceride content to one-third in the liver from A-ZIP mice (Fig. 5, *A–D*). These results indicated that hepatic AMPK activation is involved in the improvement of fatty liver by leptin in lipodystrophy. We could not find obvious decrease in the insulin levels. but the HOMA-IR tended to decrease, suggesting hepatic AMPK activation leads to improvement of insulin resistance in lipodystrophy (Fig. 5, *F* and *G*).

In conclusion, this study demonstrates that leptin activates AMPK not only in the skeletal muscle but also in the liver in mice. Leptin activates hepatic AMPK mainly through the CNS and α-adrenergic effects of sympathetic nerves. This study also indicates that hepatic AMPK is involved in the development of metabolic disorders and their improvement by leptin in A-ZIP mice. This study provides the useful notion to understand the molecular mechanism by which leptin regulates energy metabolism and will guide the development of novel metabolic pharmaceuticals.

Acknowledgments—We thank Yoko Koyama and Mayumi Nagamoto for secretarial and technical assistance and Drs. Shuichi Koda, Hideki Matsumoto, and Fumihiko Yokoya for helpful technical advice.

REFERENCES

1. Halaas, J. L., Boozer, C., Blair-West, J., Fidahusein, N., Denton, D. A., and Friedman, J. M. (1997) Physiological response to long term peripheral and central leptin infusion in lean and obese mice. *Proc. Natl. Acad. Sci. U.S.A.* **94,** 8878–8883
2. Campfield, L. A., Smith, F. J., Guisez, Y., Devos, R., and Burn, P. (1995) Recombinant mouse OB protein. Evidence for a peripheral signal linking adiposity and central neural networks. *Science* **269,** 546–549
3. Ebihara, K., Ogawa, Y., Masuzaki, H., Shintani, M., Miyanaga, F., Aizawa-Abe, M., Hayashi, T., Hosoda, K., Inoue, G., Yoshimasa, Y., Gavrilova, O., Reitman, M. L., and Nakao, K. (2001) Transgenic overexpression of leptin rescues insulin resistance and diabetes in a mouse model of lipoatrophic diabetes. *Diabetes* **50,** 1440–1448
4. Miyanaga, F., Ogawa, Y., Ebihara, K., Hidaka, S., Tanaka, T., Hayashi, S., Masuzaki, H., and Nakao, K. (2003) Leptin as an adjunct of insulin therapy in insulin-deficient diabetes. *Diabetologia* **46,** 1329–1337
5. Naito, M., Fujikura, J., Ebihara, K., Miyanaga, F., Yokoi, H., Kusakabe, T., Yamamoto, Y., Son, C., Mukoyama, M., Hosoda, K., and Nakao, K. (2011) Therapeutic impact of leptin on diabetes, diabetic complications, and longevity in insulin-deficient diabetic mice. *Diabetes* **60,** 2265–2273
6. Wang, M. Y., Chen, L., Clark, G. O., Lee, Y., Stevens, R. D., Ilkayeva, O. R., Wenner, B. R., Bain, J. R., Charron, M. J., Newgard, C. B., and Unger, R. H. (2010) Leptin therapy in insulin-deficient type I diabetes. *Proc. Natl. Acad. Sci. U.S.A.* **107,** 4813–4819
7. Shimomura, I., Hammer, R. E., Ikemoto, S., Brown, M. S., and Goldstein, J. L. (1999) Leptin reverses insulin resistance and diabetes mellitus in mice with congenital lipodystrophy. *Nature* **401,** 73–76
8. Kusakabe, T., Tanioka, H., Ebihara, K., Hirata, M., Miyamoto, L., Miyanaga, F., Hige, H., Aotani, D., Fujisawa, T., Masuzaki, H., Hosoda, K., and Nakao, K. (2009) Beneficial effects of leptin on glycaemic and lipid control in a mouse model of type 2 diabetes with increased adiposity induced by streptozotocin and a high fat diet. *Diabetologia* **52,** 675–683
9. Ebihara, K., Kusakabe, T., Hirata, M., Masuzaki, H., Miyanaga, F., Kobayashi, N., Tanaka, T., Chusho, H., Miyazawa, T., Hayashi, T., Hosoda, K., Ogawa, Y., DePaoli, A. M., Fukushima, M., and Nakao, K. (2007) Efficacy and safety of leptin-replacement therapy and possible mechanisms of leptin actions in patients with generalized lipodystrophy. *J. Clin. Endocrinol. Metab.* **92,** 532–541
10. Farooqi, I. S., Jebb, S. A., Langmack, G., Lawrence, E., Cheetham, C. H., Prentice, A. M., Hughes, I. A., McCamish, M. A., and O'Rahilly, S. (1999) Effects of recombinant leptin therapy in a child with congenital leptin deficiency. *N. Engl. J. Med.* **341,** 879–884
11. Oral, E. A., Simha, V., Ruiz, E., Andewelt, A., Premkumar, A., Snell, P., Wagner, A. J., DePaoli, A. M., Reitman, M. L., Taylor, S. I., Gorden, P., and Garg, A. (2002) Leptin replacement therapy for lipodystrophy. *N. Engl. J. Med.* **346,** 570–578
12. Petersen, K. F., Oral, E. A., Dufour, S., Befroy, D., Ariyan, C., Yu, C., Cline, G. W., DePaoli, A. M., Taylor, S. I., Gorden, P., and Shulman, G. I. (2002) Leptin reverses insulin resistance and hepatic steatosis in patients with severe lipodystrophy. *J. Clin. Invest.* **109,** 1345–1350
13. Lee, Y., Hirose, H., Ohneda, M., Johnson, J. H., McGarry, J. D., and Unger, R. H. (1994) Beta-cell lipotoxicity in the pathogenesis of non-insulin-dependent diabetes mellitus of obese rats: impairment in adipocyte-beta-cell relationships. *Proc. Natl. Acad. Sci. U.S.A.* **91,** 10878–10882
14. Perseghin, G., Scifo, P., De Cobelli, F., Pagliato, E., Battezzati, A., Arcelloni,

C., Vanzulli, A., Testolin, G., Pozza, G., Del Maschio, A., and Luzi, L. (1999) Intramyocellular triglyceride content is a determinant of *in vivo* insulin resistance in humans. A ^{1}H-^{13}C nuclear magnetic resonance spectroscopy assessment in offspring of type 2 diabetic parents. *Diabetes* **48,** 1600–1606

15. Kim, J. K., Gavrilova, O., Chen, Y., Reitman, M. L., and Shulman, G. I. (2000) Mechanism of insulin resistance in A-ZIP/F-1 fatless mice. *J. Biol. Chem.* **275,** 8456–8460
16. Minokoshi, Y., Kim, Y. B., Peroni, O. D., Fryer, L. G., Müller, C., Carling, D., and Kahn, B. B. (2002) Leptin stimulates fatty-acid oxidation by activating AMP-activated protein kinase. *Nature* **415,** 339–343
17. Winder, W. W., Wilson, H. A., Hardie, D. G., Rasmussen, B. B., Hutber, C. A., Call, G. B., Clayton, R. D., Conley, L. M., Yoon, S., and Zhou, B. (1997) Phosphorylation of rat muscle acetyl-CoA carboxylase by AMP-activated protein kinase and protein kinase A. *J. Appl. Physiol.* **82,** 219–225
18. Andreelli, F., Foretz, M., Knauf, C., Cani, P. D., Perrin, C., Iglesias, M. A., Pillot, B., Bado, A., Tronche, F., Mithieux, G., Vaulont, S., Burcelin, R., and Viollet, B. (2006) Liver adenosine monophosphate-activated kinase-α2 catalytic subunit is a key target for the control of hepatic glucose production by adiponectin and leptin but not insulin. *Endocrinology* **147,** 2432–2441
19. Assifi, M. M., Suchankova, G., Constant, S., Prentki, M., Saha, A. K., and Ruderman, N. B. (2005) AMP-activated protein kinase and coordination of hepatic fatty acid metabolism of starved/carbohydrate-refed rats. *Am. J. Physiol. Endocrinol. Metab.* **289,** E794–E800
20. Shaw, R. J., Lamia, K. A., Vasquez, D., Koo, S. H., Bardeesy, N., Depinho, R. A., Montminy, M., and Cantley, L. C. (2005) The kinase LKB1 mediates glucose homeostasis in liver and therapeutic effects of metformin. *Science* **310,** 1642–1646
21. Moitra, J., Mason, M. M., Olive, M., Krylov, D., Gavrilova, O., Marcus-Samuels, B., Feigenbaum, L., Lee, E., Aoyama, T., Eckhaus, M., Reitman, M. L., and Vinson, C. (1998) Life without white fat. A transgenic mouse. *Genes Dev.* **12,** 3168–3181
22. Ogawa, Y., Masuzaki, H., Hosoda, K., Aizawa-Abe, M., Suga, J., Suda, M., Ebihara, K., Iwai, H., Matsuoka, N., Satoh, N., Odaka, H., Kasuga, H., Fujisawa, Y., Inoue, G., Nishimura, H., Yoshimasa, Y., and Nakao, K. (1999) Increased glucose metabolism and insulin sensitivity in transgenic skinny mice overexpressing leptin. *Diabetes* **48,** 1822–1829
23. German, J., Kim, F., Schwartz, G. J., Havel, P. J., Rhodes, C. J., Schwartz, M. W., and Morton, G. J. (2009) Hypothalamic leptin signaling regulates hepatic insulin sensitivity via a neurocircuit involving the vagus nerve. *Endocrinology* **150,** 4502–4511
24. Pocai, A., Obici, S., Schwartz, G. J., and Rossetti, L. (2005) A brain-liver circuit regulates glucose homeostasis. *Cell Metab.* **1,** 53–61
25. Davies, S. P., Carling, D., Munday, M. R., and Hardie, D. G. (1992) Diurnal rhythm of phosphorylation of rat liver acetyl-CoA carboxylase by the AMP-activated protein kinase, demonstrated using freeze-clamping. Effects of high fat diets. *Eur. J. Biochem.* **203,** 615–623
26. Miyamoto, L., Toyoda, T., Hayashi, T., Yonemitsu, S., Nakano, M., Tanaka, S., Ebihara, K., Masuzaki, H., Hosoda, K., Ogawa, Y., Inoue, G., Fushiki, T., and Nakao, K. (2007) Effect of acute activation of 5′-AMP-activated protein kinase on glycogen regulation in isolated rat skeletal muscle. *J. Appl. Physiol.* **102,** 1007–1013
27. Lee, Y., Yu, X., Gonzales, F., Mangelsdorf, D. J., Wang, M. Y., Richardson, C., Witters, L. A., and Unger, R. H. (2002) PPARα is necessary for the lipopenic action of hyperleptinemia on white adipose and liver tissue. *Proc. Natl. Acad. Sci. U.S.A.* **99,** 11848–11853
28. Brabant, G., Müller, G., Horn, R., Anderwald, C., Roden, M., and Nave, H. (2005) Hepatic leptin signaling in obesity. *FASEB J.* **19,** 1048–1050
29. Dzamko, N. L., and Steinberg, G. R. (2009) AMPK-dependent hormonal regulation of whole-body energy metabolism. *Acta Physiol.* **196,** 115–127
30. Uotani, S., Abe, T., and Yamaguchi, Y. (2006) Leptin activates AMP-activated protein kinase in hepatic cells via a JAK2-dependent pathway. *Biochem. Biophys. Res. Commun.* **351,** 171–175
31. Uyama, N., Geerts, A., and Reynaert, H. (2004) Neural connections between the hypothalamus and the liver. *Anat. Rec. A Discov. Mol. Cell. Evol. Biol.* **280,** 808–820
32. Hutchinson, D. S., and Bengtsson, T. (2006) AMP-activated protein kinase activation by adrenoceptors in L6 skeletal muscle cells. Mediation by α1-adrenoceptors causing glucose uptake. *Diabetes* **55,** 682–690
33. Xu, M., Zhao, Y. T., Song, Y., Hao, T. P., Lu, Z. Z., Han, Q. D., Wang, S. Q., and Zhang, Y. Y. (2007) α1-adrenergic receptors activate AMP-activated protein kinase in rat hearts. *Sheng Li Xue Bao* **59,** 175–182
34. Koh, H. J., Hirshman, M. F., He, H., Li, Y., Manabe, Y., Balschi, J. A., and Goodyear, L. J. (2007) Adrenaline is a critical mediator of acute exercise-induced AMP-activated protein kinase activation in adipocytes. *Biochem. J.* **403,** 473–481
35. Barnes, B. R., Ryder, J. W., Steiler, T. L., Fryer, L. G., Carling, D., and Zierath, J. R. (2002) Isoform-specific regulation of 5′-AMP-activated protein kinase in skeletal muscle from obese Zucker (fa/fa) rats in response to contraction. *Diabetes* **51,** 2703–2708
36. Bergeron, R., Previs, S. F., Cline, G. W., Perret, P., Russell, R. R., 3rd, Young, L. H., and Shulman, G. I. (2001) Effect of 5-aminoimidazole-4-carboxamide-1-β-D-ribofuranoside infusion on *in vivo* glucose and lipid metabolism in lean and obese Zucker rats. *Diabetes* **50,** 1076–1082
37. Yu, X., McCorkle, S., Wang, M., Lee, Y., Li, J., Saha, A. K., Unger, R. H., and Ruderman, N. B. (2004) Leptinomimetic effects of the AMP kinase activator 5-aminoimidazole-4-carboxamide 1-β-D-ribofuranoside (*AICAR*) in leptin-resistant rats: prevention of diabetes and ectopic lipid deposition. *Diabetologia* **47,** 2012–2021
38. Cool, B., Zinker, B., Chiou, W., Kifle, L., Cao, N., Perham, M., Dickinson, R., Adler, A., Gagne, G., Iyengar, R., Zhao, G., Marsh, K., Kym, P., Jung, P., Camp, H. S., and Frevert, E. (2006) Identification and characterization of a small molecule AMPK activator that treats key components of type 2 diabetes and the metabolic syndrome. *Cell Metab.* **3,** 403–416

INTERNAL MEDICINE

□ CASE REPORT □

Premature Atherosclerosis in a Japanese Diabetic Patient with Atypical Familial Partial Lipodystrophy and Hypertriglyceridemia

Masanori Iwanishi[1], Ken Ebihara[2], Toru Kusakabe[2], Shinji Harada[1], Jun Ito-Kobayashi[1], Atsushi Tsuji[3], Kiminori Hosoda[2] and Kazuwa Nakao[2]

Abstract

We herein report a case of premature atherosclerosis in a patient with familial partial lipodystrophy (FPL), diabetes mellitus, hypertension and hypertriglyceridemia. Sequencing of the candidate genes *LMNA*, *PPARG* and *CAV1* associated with FPL revealed no genetic abnormalities, which indicated the activity of a novel gene in this patient. The patient's son showed milder fat loss and similar fat distribution compared to the proband; however, the son showed no signs of any atherosclerotic disease. Although a cluster of atherogenic risk factors is likely to be the primary causes of atherosclerosis in our patient, other factors, including an unknown gene associated with FPL, the severity of fat loss and gender, might affect the development of atherosclerosis.

Key words: familial partial lipodystrophy (FPL), premature atherosclerosis, insulin resistance, pioglitazone

(Intern Med 51: 2573-2579, 2012)
(DOI: 10.2169/internalmedicine.51.7461)

Introduction

Lipodystrophies are a heterogeneous group of diseases characterized by generalized or partial fat loss (1-5). Some patients with partial lipodystrophies show fat hypertrophy in other locations. Lipodystrophy is diagnosed on the basis of fat loss in portions of the body determined with dual energy X-ray absorptiometry (DEXA) and magnetic resonance imaging (MRI) scans. Lipodystrophies are rare and have both inherited and acquired forms. Acquired lipodystrophies can be generalized or partial. Although the causes of acquired lipodystrophies are generally unknown, such acquired lipodystrophies can be associated with signs of autoimmunity. Patients with lipodystrophies often also have a cluster of associated diseases, including insulin resistance, dyslipidemia, hypertension, fatty liver and diabetes, similar to that observed in patients with metabolic syndrome. These patients often die of health problems, including ischemic heart disease, cerebral infarction, renal failure, severe liver dysfunction and pancreatitis. Congenital generalized lipodystrophies (CGLs) are autosomal recessive disorders that, in most patients, result from mutations in the genes encoding Seipin and 1-acylglycerol-3-phosphate-O-acyltransferase 2 (AGPAT2) (6). Familial partial lipodystrophies (FPLs) are autosomal dominant disorders, and mutations in the genes encoding laminin A/C, peroxisome proliferator-activated receptor-γ (PPARG) or caveolin have been reported in patients with FPL. Familial partial lipodystrophy, Dunnigan variety (FPLD) is named after Dunnigan, who provided a detailed description of the syndrome (7). FPLD is associated with several mutations in the genes encoding laminin A/C. However, a number of patients with FPL remain undiagnosed at the genetic level.

Women with FPLD have a higher prevalence of diabetes and atherosclerotic vascular disease, higher serum triglyceride (TG) levels and lower high-density lipoprotein (HDL) cholesterol concentrations than men with FPLD (3, 9). However, some patients with CGL or FPL do not have overt atherosclerotic diseases. Furthermore, the evidence for pre-

[1]Diabetes and Endocrine Division, Kusatsu General Hospital, Japan, [2]Department of Medicine and Clinical Science, Kyoto University Graduate School of Medicine, Japan and [3]Department of Neurosurgery, Kusatsu General Hospital, Japan
Received for publication February 8, 2012; Accepted for publication June 7, 2012
Correspondence to Dr. Masanori Iwanishi, masa-iwani@solid.ocn.ne.jp

Table 1. Biochemical Data of This Family

Metabolic variables		Patient 1	Patient 2	Normal values	
Plasma glucose		154	86	70-109	(mg/dL)
HbA1c		6.5	4.8	4.3-5.8	(%)
plasma insulin			5.6	2.2-12.4	(μU/mL)
plasma CPR		2.0		0.7-3.5	(ng/dL)
Serum triglycerides		755	125	35-149	(mg/dL)
Serum cholesterol		211	151	130-219	(mg/dL)
Serum HDL cholesterol		34	40	40-83	(mg/mL)
Serum leptin		36.1	3.9		(ng/mL)
Serum adiponectin		7.1	5.7		(μg/mL)
Urinary CPR	2003	68.7			(μg/day)
	2005	74.8			
	2007	10			

mature atherosclerosis in patients with CGL or other forms of FPL is minimal, probably because the number of patients with these conditions is small. The mechanisms underlying the development of atherosclerosis in patients with FPL remain unknown. Therefore, in this case report, we include the clinical findings and results of a genetic analysis for our patient in order to clarify the mechanisms underlying atherosclerosis in FPL.

Case Report

The patient was a 48-year-old woman. When she was 16 years old, she had a body mass index (BMI) of 36.5, which indicated obesity. At 35 years of age, she was diagnosed with diabetes by a family doctor based on the presence of high levels of hemoglobin A1c (HbA1c) and postprandial glucose. Her diabetes remained uncontrolled (HbA1c level: 8.0%-12.0%) despite treatment with a combination of 10 mg of glibenclamide and 0.6 mg of voglibose. At 40 years of age, she was transferred to the hospital emergency room due to convulsions and a disturbance of consciousness. Her magnetic resonance imaging (MRI, left panel) and magnetic resonance angiography (MRA, right panel) findings showed severe narrowing at the end of the internal carotid artery on both sides with an old cerebral infarction in the right anterior lobe (Fig. 3A, B). The narrowing in the proximal region of the anterior and middle cerebral arteries on both sides is indicated by arrows. The presence of lesions suggested a diagnosis of premature atherosclerosis, because the patient had multiple atherogenic risk factors, including diabetes mellitus, hypertension and hypertriglyceridemia. However, we could not completely rule out moyamoya disease, because we did not perform a biopsy of the lesions that narrowed the arterial wall (10). We initiated treatment with 160 mg of valsartan and 40 mg of Adalat-CR for hypertension in 2003 when the patient was 43 years old. Her blood pressure was reduced to 130/50 mmHg. Subsequently, superficial temporal artery-middle cerebral artery (STA-MCA) anastomosis was performed. The patient was admitted to our hospital for diabetes care in May 2007 when she was 48 years old. At that time, her height was 152 cm and she weighed 64 kg, which indicated a body mass index of 27.2. She did not have a history of either autoimmune or infectious diseases. She did not have a habit of smoking or consuming alcohol. She had entered menopause at the age of 40. Her HbA1c concentration was 6.5% (Table 1) and although her blood glucose level was found to be satisfactory on her first visit to our hospital, her dose of insulin was increased to 72 U/day (1.1 U/kg/day). Her serum TG level was 755 mg/dL and her HDL cholesterol level was 34 mg/dL; however, her blood glucose level was well-controlled. This suggested that the hypertriglyceridemia was due to insulin resistance. The patient did not have any other abnormal endocrinological findings, including abnormal cortisol levels. Her serum leptin level was 36.1 ng/mL, while her serum adiponectin level was 7.1 μg/mL. Her urinary C peptide level was 68.7 μg/day in 2003, 74.8 μg/day in 2005 and 10 μg/day in 2007. This observation indicated a recent deterioration in insulin deficiency despite the relatively conserved insulin levels observed in 2003 and 2005. The patient had mild nonproliferative diabetic retinopathy. Her total urinary protein level was 1.0 g/day and her serum creatinine level was 1.06 mg/dL, which indicated overt diabetic nephropathy. An abdominal echo showed mild fatty liver and the L/S ratio of the computed tomography (CT) value was 1.3. The patient's serum albumin level, platelet count and hyaluronic acid level were within normal limits, which suggested that she did not have severe non-alcoholic steatosis hepatitis. She had noticed a loss of subcutaneous fat over her forearms, lower limbs and buttocks at 12 years of age. On admission, she showed loss of subcutaneous fat deposits in the forearms (right panel), lower limbs and buttocks, with prominent lower limb musculature and excess fat deposition around the face, neck and trunk (left panel, Fig. 1B). The patient's mother and son showed a similar distribution of fat atrophy and we therefore considered an autosomal dominant pattern of inheritance (Fig. 1A). The patient's condition was clinically diagnosed as FPL. The patient's mother was diagnosed with diabetes at 31 years of age and died of a cerebral infarction at 38 years of age. The patient's father died of chronic renal failure at the age of 75 and was not evaluated for fat atrophy or glucose tolerance. We assessed body fat distribution in the proband (Patient 1) in 2007 using DEXA and MRI studies. Thoracic (left panel) and abdominal MRI (right panel) revealed preservation of subcutaneous fat in the abdominal and thoracic regions (Fig. 2A). MRI images obtained at the level of the gluteal fat revealed a marked loss of gluteal subcutaneous fat (Fig. 2B). Axial MRI performed at the level of the thigh (upper panel) and calf (lower panel) revealed a marked loss of subcutaneous fat in these regions (Fig. 2C). Patient 1 had decreased amounts of subcutaneous fat, particularly in the antero-lateral and posterior thigh and calf regions. Axial MRI performed at the level of the forearms (lower panel) revealed almost a complete absence of subcutaneous fat in the forearms, while axial MRI performed at the level of the arms (upper panel) revealed the preservation of subcutaneous fat in this region (Fig. 2D).

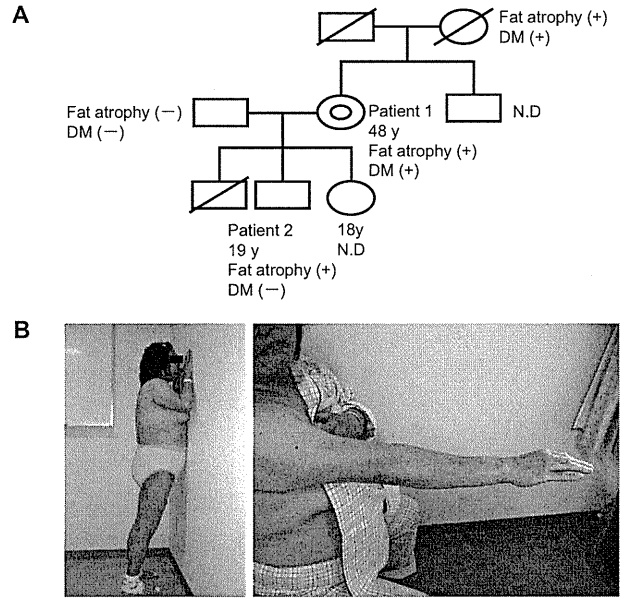

Figure 1. A. The pedigree of a Japanese family with lipodystrophy. While the proband (Patient 1) and her mother exhibited marked losses of subcutaneous fat in the lower limbs and buttocks, the son (Patient 2) exhibited only a moderate loss of subcutaneous fat. The proband and her mother both had diabetes mellitus. B. The phenotypic features of Patient 1 are shown in the left panel. Note the prominent musculature of the lower limbs as well as the preservation of abdominal and cervical fat and the loss of fat in the lower limbs and gluteal tissues. The right panel shows fat atrophy in the forearms and conservation of subcutaneous fat in the arms.

The area of visceral fat located at the umbilical level measured 140.4 cm^2. The regional and whole-body adipose tissue distribution and body composition estimated by the DEXA scan is shown in Table 2. Compared to normal subjects, Patient 1 had markedly lower levels of fat in her legs, with prominent accumulation of fat in the trunk. She appeared to have well-preserved skeletal muscle.

The son of Patient 1 (Patient 2) was a 19-year-old man. His height was 163 cm and weight was 86.8 kg, thus suggesting a body mass index of 32.7. His blood pressure showed a normal range, and he did not have any health problems except for obesity. We assessed fat atrophy in various regions in Patient 2 using a DEXA scan and CT. As shown in Table 2, we evaluated fat mass compared with two controls. The average BMI in Control Group 2, which included 72 healthy men between the ages of 20 and 29, was 22.4, while that in Control Group 3, which included 11 healthy men between the ages of 20 and 29, was 26.4. The finding of a BMI in Patient 2 of 32.7 kg/m^2 indicated that % fat and fat mass in one leg was relatively low, which suggested fat atrophy in the legs. The CT images of Patient 2 showed relatively low levels of subcutaneous fat in the thigh and buttocks (Fig. 4). Patient 2 had a marked loss of subcutaneous fat, particularly in the lateral thigh, calf and forearm regions. Patients with FPL show marked losses of subcutaneous fat, particularly in the lateral thigh and calf regions (3). Therefore, the fat distribution pattern observed in Patient 2 seemed to be similar to that of his mother (Patient 1) and was consistent with the above observations. The area of visceral fat located at the umbilical level measured 69.5 cm^2. Patient 2's fasting serum TG level was 125 mg/dL and his HbA1c level was 4.8%, both of which were within normal limits. An oral glucose tolerance test (OGTT) showed that Patient 2's blood glucose levels were 86, 111, 133 and 118 mg/dL, while his insulin levels were 5.6, 36.2, 92.9 and 68.8 μU/mL at 0, 30, 60 and 120 minutes. Therefore, the OGTT showed normal glucose levels with relatively high insulin levels. Both brain MRI and MRA showed normal results (data not shown). Therefore, Patient 2 did not have visceral obesity, hypertriglyceridemia, diabetes mellitus, hypertension or premature atherosclerosis, although he seemed to have partial lipodystrophy.

We examined the effects of pioglitazone on the metabolic values and the changes in lean mass and fat mass regions in Patient 1. We prescribed pioglitazone (15 mg/day) because thiazolidinediones have been reported to be effective for glycemic control in patients with FPL. We examined Patient 1's response to pioglitazone by monitoring her HbA1c levels and the changes in her biochemical data, body weight, fat and lean mass during treatment using DEXA. After three months of treatment, Patient 1's HbA1c level decreased from 9.2% to 7.1% and remained at approximately 7.0% thereafter, while her serum TG level decreased from 1,102 mg/dL to 431 mg/dL. After two weeks of pioglitazone treatment, the dose of insulin was reduced to 18 U/day (0.26 U/kg/day). After three months, Patient 1's body weight increased from 67.0 to 78.0 kg. We decreased the dose of pioglitazone to 7.5 mg to prevent additional gains in body weight. The changes in fat and lean mass were monitored during pioglitazone treatment using DEXA scans. In addition, we evaluated the changes in the leptin and adiponectin levels during pioglitazone treatment. A comparison of the results of the DEXA scans showed that the fat mass increased by 2.6 kg, while the lean mass increased by 6.5 kg during pioglitazone treatment. Pioglitazone induced increases in fat mass predominantly in the trunk, and no increases were detectable in the lower limbs. After three months of treatment, the serum adiponectin level increased from 7.1 to 24.0 μg/mL and the HDL cholesterol level increased from 34 mg/dL to 45 mg/dL.

We examined the sequences of the entire coding region and the exon-intron boundary regions of the *LMNA*, *PPARG* and *CAV1* genes, which are known to be associated with FPL; however, we found no mutations in these genes in the proband.

Discussion

We herein report the case of a 48-year-old Japanese woman (Patient 1) with diabetes and atypical FPL who showed marked losses of subcutaneous fat in the forearms, lower limbs and buttocks. The fat distribution pattern ob-

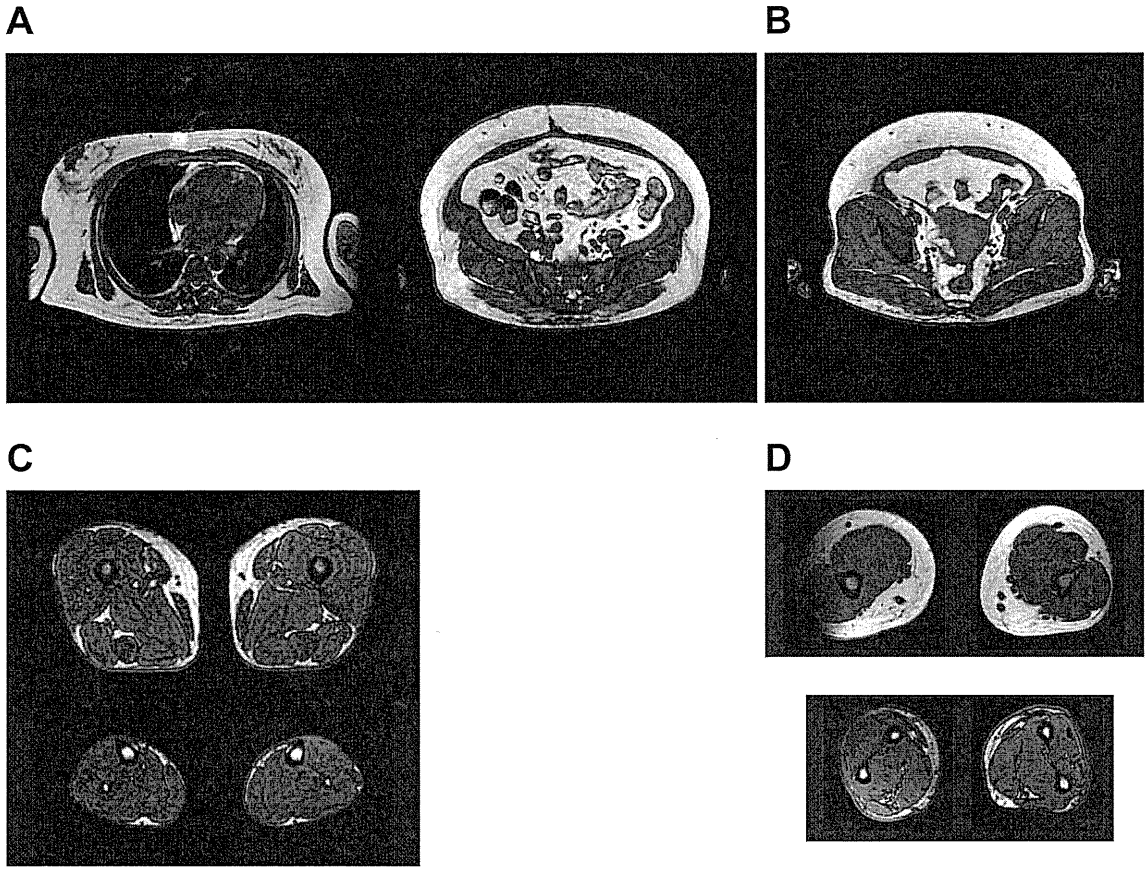

Figure 2. The figure shows magnetic resonance imaging (MRI) results for Patient 1. A. Thoracic MRI images taken at the level of the fourth thoracic vertebrae (left panel) and abdominal MRI images taken at the umbilical level (right panel) showed the preservation of subcutaneous fat in the thoracic and abdominal regions. B. A T1-weighted MRI image taken at the level of the gluteal fat indicated a striking loss of gluteal subcutaneous fat. C. MRI images taken at the level of the thigh (upper panel) and calf (lower panel) revealed a nearly complete absence of subcutaneous fat. Patient 1 had decreased amounts of subcutaneous fat, particularly in the antero-lateral and posterior thigh and calf regions. D. MRI images taken at the level of the arms (upper panel) and forearms (lower panel) revealed a marked loss of subcutaneous fat in the forearms and preservation of fat in the arms.

served in Patient 1 seemed to be similar to that seen in patients with atypical partial lipodystrophy with *PPARG* mutations (11-13).

Patient 1 had been severely obese since 16 years of age. Her abdominal CT images showed visceral obesity. The age of onset of diabetes mellitus in Patient 1 was 35 years, which was relatively early compared to that observed in patients with type 2 diabetes mellitus. At 40 years of age, Patient 1 showed severe narrowing at the end of the internal carotid artery on both sides with an old cerebral infarction in the right anterior lobe, which suggested the presence of premature atherosclerosis. Because Patient 1 had visceral obesity and FPL, her intra-hepatic and intra-myocellular lipid contents may have been increased, which may have caused greater insulin resistance and worsened the atherosclerosis. The serum adiponectin levels are thought to be associated with the indices of insulin resistance and atherosclerosis (14, 15). Patient 1's serum adiponectin level was 7.1 μg/mL. The data suggested that Patient 1's serum adiponectin levels were relatively lower than those in 28 women with normal glucose tolerance (16). The level of adiponectin may also have had an effect on atherosclerosis in the case of Patient 1. Women with FPLD have a higher prevalence of diabetes and atherosclerotic vascular disease, higher serum TG levels and lower HDL cholesterol concentrations than men with FPLD (3, 9). Therefore, because Patient 1 was a woman with FPL and had a cluster of atherogenic risk factors, including diabetes mellitus, hypertension and hypertriglyceridemia, she had a predisposition for developing atherosclerosis. On the other hand, her son did not have premature atherosclerosis. The reasons for this were thought to be as follows: first, Patient 1's son was a 19-year-old man with a less severe amount of fat loss compared to his mother; second, he did not have hypertriglyceridemia, hypertension or diabetes mellitus, although he did have insulin resistance. We previously reported the case of a Japanese woman with diabetes with atypical FPL who had normal serum TG levels and did not have overt atherosclerosis (17).

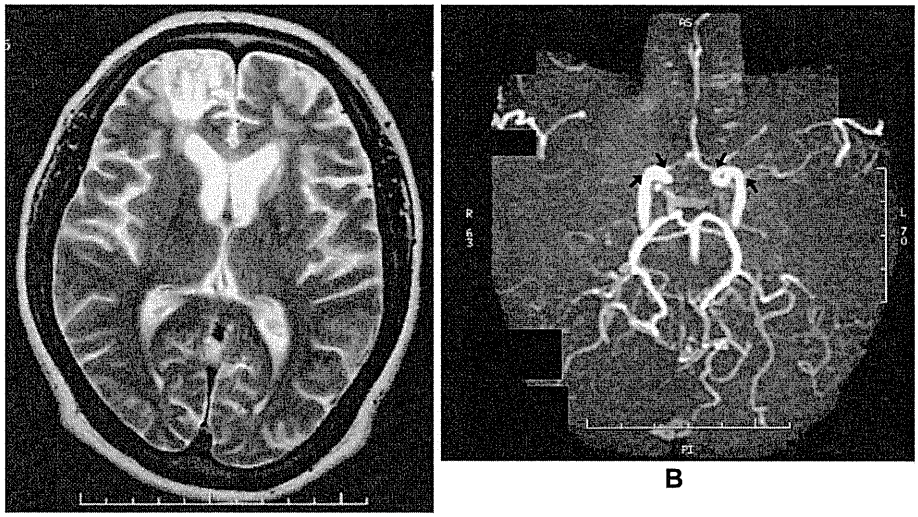

Figure 3. Brain magnetic resonance imaging (MRI), which had been performed when Patient 1 was transferred to the emergency room for convulsions at 40 years of age, showed an old infarction in the right frontal lobe (left panel), while brain magnetic resonance angiography (MRA) showed severe narrowing in the end of both sides of the internal carotid artery (right panel). The narrowing in the proximal region of both sides of the anterior cerebral and middle cerebral arteries is indicated by arrows.

Table 2. Body Composition as Determined by DEXA Scan in the Patient 1 and the Patient 2

	Patient 1	Control 1	Patient 2	Control 2	Control 3
Height (cm)	152.0	156.1 ± 4.9	163.0	172.2 ± 5.3	170.4 ± 4.0
Body weight (kg)	69.0	55.1 ± 6.7	86.8	66.4 ± 9.9	80.4 ± 8.7
BMI (kg/m^2)	30.0	22.7 ± 3.0	32.7	22.4 ± 3.2	27.7 ± 2.6
Age (years)	48	45.1 ± 2.8	19	25.6 ± 2.7	26.4 ± 1.8
1) Fat (%)					
whole body	31.6	30.3 ± 6.2	25.7	15.6 ± 9.5	25.6 ± 6.2
one arm	46.4	26.9 ± 7.3	30.6	11.9 ± 5.9	20.1 ± 6.4
one leg	15.4	33.2 ± 5.7	20.3	16.3 ± 6.4	25.0 ± 5.6
trunk	37.9	28.4 ± 7.7	27.9	15.7 ± 8.3	27.3 ± 7.3
2) Fat Mass (kg)					
whole body	23.8	16.8 ± 5.2	19.3	10.8 ± 6.4	20.7 ± 6.8
one arm	1.5	0.7 ± 0.3	1.6	0.4 ± 0.3	0.8 ± 0.3
one leg	1.1	3.5 ± 1.0	2.7	2.2 ± 1.1	3.9 ± 1.1
trunk	15.0	7.1 ± 2.8	10.8	4.8 ± 3.4	10.0 ± 4.0
3) Lean Mass (kg)					
whole body	49.0	35.3 ± 3.1	53.7	52.0 ± 5.4	55.5 ± 0.2
one arm	1.7	1.7 ± 0.2	3.5	2.7 ± 0.4	2.9 ± 0.3
one leg	5.9	6.6 ± 0.9	10.0	10.2 ± 1.6	10.9 ± 1.4
trunk	23.9	16.3 ± 1.3	27.3	22.7 ± 2.3	24.6 ± 2.5

※ Normal values in control 1 are obtained from 55 healthy women between the ages of 40 years and 49 years. Normal values in control 2 are obtained from 72 healthy men between the ages of 20 years and 29 years, while ones in control 3 are obtained from 11 healthy men between ages of 20 years and 29 years. Fat(%), Fat mass and Lean mass in one arm and leg indicates the mean values of left and right arm (or leg).

Therefore, the severity of atherosclerosis in women with FPL seems to be variable, although the evidence for accelerated atherosclerosis in patients with FPL is minimal.

Hegele RA has also reported FPLD with the *LMNA* codon 482 mutation to be associated with an increased risk of developing early coronary heart disease (8). In that report, the author speculated that *LMNA* mutations within arterial walls may affect the progression of atherosclerosis. In addition, we can speculate that an unidentified gene may affect arterial walls, which may have accelerated the progression of atherosclerosis in the case of Patient 1.

Dyslipidemia is common in insulin resistance and is characterized by fasting hypertriglyceridemia, low levels of HDL cholesterol and a delayed clearance of TG-rich lipoproteins, including very low density lipoproteins (VLDLs) (18, 19). Recently, the mechanisms underlying the development of hypertriglyceridemia in patients with general and partial lipodystrophies have been reported (20, 21). Hepatic VLDL

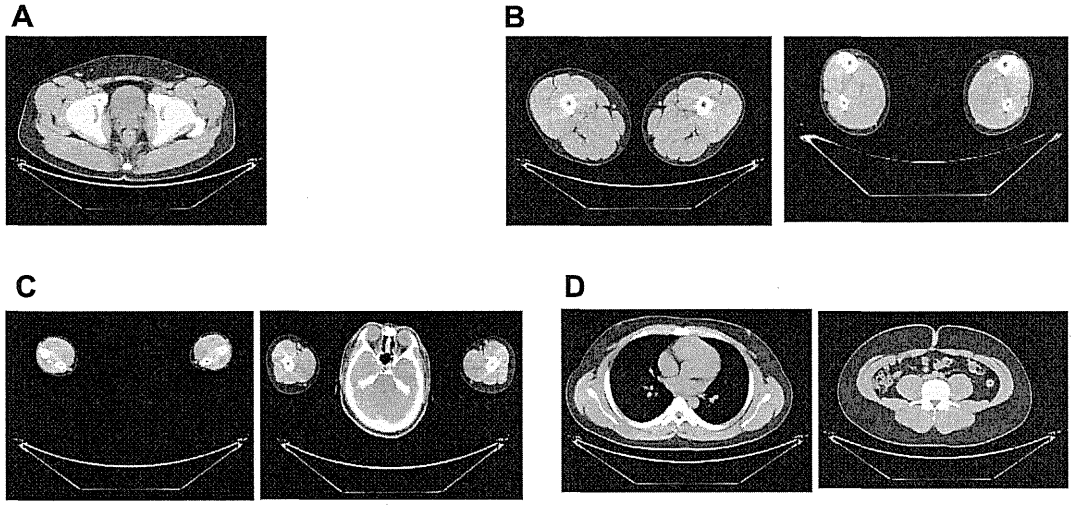

Figure 4. Computed tomography (CT) images of various regions of the patient's son (Patient 2) were obtained to evaluate fat distribution. A. CT images taken at the level of the gluteal fat were obtained. B. CT images taken at the level of the thigh are shown in the left panel, while images taken at the level of the calf are shown in the right panel. Patient 2 had decreased amounts of subcutaneous fat, particularly in the lateral thigh and calf regions. C. CT images taken at the level of the forearms are shown in the left panel, while images taken at the level of the arms are shown in the right panel. Patient 2 had decreased amounts of subcutaneous fat, particularly in the lateral forearms. D. Thoracic CT images taken at the level of the fourth thoracic vertebrae are shown in the left panel, while abdominal CT images taken at the umbilical level are shown in the right panel.

production increases in patients with insulin resistance and partial lipodystrophy. In the case of Patient 1, the serum levels of fasting TG, apolipoprotein C2, C3 and E were high (data not shown), which indicated a high concentration of VLDLs in the blood. Such high levels of VLDLs cause increases in *de novo* lipogenesis in the liver. Therefore, the presence of VLDL remnants may be the primary cause of accelerated atherosclerosis in Patient 1.

Although the effects of thiazolidinediones on glycemic control appear to vary in patients with FPL (11, 17, 22-26), pioglitazone treatment decreased the levels of HbA1c and fasting TG in the case of Patient 1. It is conceivable that pioglitazone improves glycemic control and triglycemic control by reducing the levels of free fatty acids (FFA) in venous effluent from adipose tissue and by limiting the lipotoxicity of other insulin-sensitive tissues, e.g. the liver and muscle (27, 28). In Patient 1, pioglitazone not only increased fat mass, but also increased lean mass. Although the significance of increased lean mass is not known, we might speculate that pioglitazone improves glycemic control not only by inducing adipocyte differentiation, but also by increasing the lean mass.

In conclusion, we herein described a case of premature atherosclerosis in a Japanese diabetic patient with atypical FPL and hypertriglyceridemia. Pioglitazone was effective in controlling the blood glucose levels, TG and adiponectin. In this case, the sequencing of candidate genes *LMNA*, *PPARG* and *CAV1*, which are known to be associated with FPL, revealed no genetic abnormalities and therefore suggested that a novel gene may be involved. Although a cluster of atherogenic risk factors in a woman with FPL is likely to play a major role in atherosclerosis, other factors, including genes associated with FPL, might affect the development of atherosclerosis. Further studies should be performed in order to obtain additional clinical and genetic information to better understand the mechanisms underlying premature atherosclerosis in patients with FPL.

The authors state that they have no Conflict of Interest (COI).

Acknowledgement

We thank Dr Takashi Shiokawa (Tanita Inc, Tokyo, Japan) for providing the DEXA data of 55 healthy women between the ages of 40 and 49, and of 72 healthy men between the ages of 20 and 29.

References

1. Semple RK, Krishna V, Chatterjee K, O'Rahilly S. PPARG and human metabolic disease. J Clin Invest **116**: 581-589, 2006.
2. Agarwal AK, Garg A. Genetic disorders of adipose tissue development, differentiation and death. Annu Rev Genomics Hum Genet **7**: 175-199, 2006.
3. Agarwal AK, Garg A. Genetic basis of lipodystrophies and management of metabolic complications. Annu Rev Med **57**: 297-311, 2006.
4. Kim SK, Park SW, Hwang IJ, Lee YK, Cho YW. High fat stores in ectopic compartments in men with newly diagnosed type 2 diabetes: an anthropometric determinant of carotid atherosclerosis and insulin resistance. International Journal of Obesity **34**: 105-110, 2010.
5. Garg A. Lipodystrophies: Genetic and acquired body fat disorders. J Clin Endocrinol Metab **96**: 3313-3325, 2011.

6. Ebihara K, Kusakabe T, Masuzaki H, et al. Genes and phenotype analysis of congenital generalized lipodystrophy in Japanese: a novel homozygous nonsense mutation in seipin gene. J Clin Endocrinol Metab **89**: 2360-2364, 2004.
7. Dunnigan MG, Cochrane MA, Kelly A, Scott JW. Familial lipoatrophic diabetes with dominant transmission. Quarterly Journal of Medicine **169**: 33-48, 1974.
8. Hegele RA. Premature atherosclerosis associated with monogenic insulin resistance. Criculation **103**: 2225-2229, 2001.
9. Garg A. Gender differences in the prevalence of metabolic complications in familial partial lipodystrophy (Dunnigan variety). J Clin Endocrinol Metab **85**: 1776, 2000.
10. Pollak L. Mayamoya disease and moyamoya syndrome. N Engl J Med **260**: 1226-1237, 2009.
11. Savage DB, Tan GD, Acerini CL, et al. Human metabolic syndrome resulting from dominant-negative mutations in the nuclear receptor peroxisome proliferator-activated receptor-G. Diabetes **52**: 910-917, 2003.
12. Hegele RA, Cao H, Frankowski C, Mathews S, Leff T. PPARG F 388L, a transactivation-deficient mutant, in familial partial lipodystrophy. Dabetes **51**: 3586-3590, 2002.
13. Agarwal AK, Grag A. A novel heterozygous mutation in peroxisom proliferator-activates receptor-G gene in a patient with familial partial lipodystrophy. J Clin Endorinol Metab **87**: 408-411, 2002.
14. Haque WA, Shimomura I, Matsuzawa Y, Garg A. Serum adiponectin and leptin levels in patients in patients with lipodystrophies. J Clin Endocrinol Metab **87**: 2395-2398, 2002.
15. Cook JR, Semple RK. Hypoadiponectinemia-cause or consequence of human insulin resistance? J Clin Endocrinol Metab **95**: 1544-1554, 2010.
16. Hotta K, Funahashi T, Arita Y, et al. Plasma concentrations of a novel, adipose-specific protein, adiponectin, in type 2 diabetic patients. Arterioscler Thromb Vasc Biol **20**: 1595-1599, 2000.
17. Iwanishi M, Ebihara K, Kusakabe T, et al. Clinical characteristics and efficacy of pioglitazone in a Japanese diabetic patient with an unusual type of familial partial lipodystrophy. Metabolism **58**: 1681-1687, 2009.
18. Ginsberg HN, Zhang YL, Hernandea-Ono A. Regulation of plasma triglycerides in insulin resistance and diabetes. Archives of Medical Research **36**: 232-240, 2005.
19. Adiel M, Taskinen MR, Boren J. Fatty liver, insulin resistance and dyslipidemia current diabetes reports. **8**: 60-64, 2008.
20. Simha V, Garg A. Inherited lipodystrophies and hypertriglyceridemia. Current Opinion in Lipodology **20**: 300-308, 2009.
21. Semple RK, Sleigh A, Murgatroyd PR, et al. Post receptor insulin resistance contributes to human dyslipidemia and hepatic steatosis. J Clin Invest **119**: 315-322, 2009.
22. Arioglu EA, Duncan-Morin J, Sebring N, et al. Efficacy and safety of troglitazone in the treatment of lipodystrophy syndromes. Ann Intern Med **133**: 263-274, 2000.
23. Owen KR, Donohoe M, Ellard S, Hattersley AT. Response to treatment with rosiglitazone in familial partial lipodystrophy due to a mutation in the LMNA gene. Diabet Med **20**: 823-827, 2003.
24. Sleilati GG, Leff T, Bonnett JW, Hegele R. Efficacy and safety of pioglitazone in treatment of a patient with an atypical lipodystrophy syndrome. Endocri Pract **13**: 656-661, 2007.
25. Ludtke A, Heckt K, Geneschel J, et al. Long-term treatment experience in a subject with Dunnigan-type familial partial lipodystrophy: efficacy of rosiglitazone. Diabet Med **22**: 1611-1613, 2005.
26. Gaudillat CC, Bancel AB, Beressi JP. Long-term improvement of metabolic control with pioglitazone in a woman with diabetes mellitus related to Dunigan syndrome: A case report. Diabetes Metab **35**: 151-154, 2009.
27. Majal KA, Cooper MB, Luc SG, Taskinen MR, Betteridge DJ. The effect of sensitization to insulin with pioglitazone on fasting and postprandial lipid metabolism, lipoprotein modification by lipases, and lipid transfer activites in type 2 diabetic patients. Diabetologia **49**: 527-537, 2006.
28. Ynag X, Smith U. Adipose tissue distribution and risk of metabolic disease: does thiazolidinedione-induced adipose tissue redistribution provide a clue to the answer? Diabetologia **50**: 1127-1133, 2007.

Functional Magnetic Resonance Imaging Analysis of Food-Related Brain Activity in Patients with Lipodystrophy Undergoing Leptin Replacement Therapy

Daisuke Aotani, Ken Ebihara, Nobukatsu Sawamoto, Toru Kusakabe, Megumi Aizawa-Abe, Sachiko Kataoka, Takeru Sakai, Hitomi Iogawa, Chihiro Ebihara, Junji Fujikura, Kiminori Hosoda, Hidenao Fukuyama, and Kazuwa Nakao

Department of Medicine and Clinical Science (D.A., K.E., T.K., M.A.-A., S.K., T.S., H.I., C.E., J.F., K.H., K.N.), Kyoto University Graduate School of Medicine, Department of Experimental Therapeutics (D.A., K.E., M.A.-A., K.H.), Translational Research Center, Kyoto University Hospital; and Kyoto University Graduate School of Medicine, Human Brain Research Center (N.S., H.F.), Kyoto 606-8507, Japan

Context: Lipodystrophy is a disease characterized by a paucity of adipose tissue and low circulating concentrations of adipocyte-derived leptin. Leptin-replacement therapy improves eating and metabolic disorders in patients with lipodystrophy.

Objective: The aim of the study was to clarify the pathogenic mechanism of eating disorders in lipodystrophic patients and the action mechanism of leptin on appetite regulation.

Subjects and Interventions: We investigated food-related neural activity using functional magnetic resonance imaging in lipodystrophic patients with or without leptin replacement therapy and in healthy controls. We also measured the subjective feelings of appetite.

Results: Although there was little difference in the enhancement of neural activity by food stimuli between patients and controls under fasting, postprandial suppression of neural activity was insufficient in many regions of interest including amygdala, insula, nucleus accumbens, caudate, putamen, and globus pallidus in patients when compared with controls. Leptin treatment effectively suppressed postprandial neural activity in many of these regions of interest, whereas it showed little effect under fasting in patients. Consistent with these results, postprandial formation of satiety feeling was insufficient in patients when compared with controls, which was effectively reinforced by leptin treatment.

Conclusions: This study demonstrated the insufficiency of postprandial suppression of food-related neural activity and formation of satiety feeling in lipodystrophic patients, which was effectively restored by leptin. The findings in this study emphasize the important pathological role of leptin in eating disorders in lipodystrophy and provide a clue to understanding the action mechanism of leptin in human, which may lead to development of novel strategies for prevention and treatment of obesity. (*J Clin Endocrinol Metab* 97: 3663–3671, 2012)

Lipodystrophy is a disease characterized by a paucity of adipose tissue due to genetic or acquired conditions that alter the ability to store triglyceride in adipose tissue (1–4). Patients with lipodystrophy have abnormally low circulating concentrations of adipocyte-derived leptin and frequently develop a wide range of met-

ISSN Print 0021-972X ISSN Online 1945-7197
Printed in U.S.A.

doi: 10.1210/jc.2012-1872 Received April 4, 2012. Accepted July 18, 2012.
First Published Online August 7, 2012

Abbreviations: BMI, Body mass index; CGL, congenital generalized lipodystrophy; FDR, false discovery rate; fMRI, functional magnetic resonance imaging; ROI, region of interest; VAS, visual analog scale.

abolic disorders including insulin-resistant diabetes, hypertriglyceridemia, and fatty liver (1, 5, 6). Lipodystropic patients also exhibit eating disorders, which makes diet therapy difficult (7).

We and others have demonstrated that leptin-replacement therapy effectively improves metabolic disorders in patients with lipodystrophy (1, 8, 9). In this context, leptin was also shown to suppress appetite in lipodystrophic patients (7, 10). Leptin treatment decreased satiation time, *i.e.* the time to voluntary cessation of eating, and increased satiety time, *i.e.* the time to hunger sufficient to consume a full meal. However, there is no report on the comparison of eating behaviors between healthy subjects and patients with lipodystrophy. Therefore, the pathophysiological role of leptin in eating disorders in patients with lipodystrophy remains unclear.

Leptin is a hormone secreted by the adipocytes, which serves to communicate the status of body energy store to the central nervous system and controls eating behavior and energy expenditure (11–16). From experimental studies in human and animals, it has long been established that leptin suppresses energy intake mainly by acting on the hypothalamus (7, 17, 18). However, there is little information about how the neural networks including the hypothalamus are influenced by leptin signals. Recently the advent of functional neuroimaging techniques such as functional magnetic resonance imaging (fMRI) has been providing novel insights into homeostatic and hedonic aspects of human eating behavior. fMRI measurements of food-related neural activity in congenital leptin-deficient patients were reported (19–21). These studies revealed that leptin treatment modulates neural activity in reward- and food-related areas such as the ventral striatum and orbitofrontal cortex.

In the present study, to reveal the pathogenic mechanism of eating disorders in lipodystrophic patients, we measured food-related neural activity by fMRI scans and investigated subjective feelings of appetite under both fasting and postprandial conditions in patients and age- and sex-matched healthy subjects. In addition, we performed the same sequential analyses in the same patients with leptin-replacement therapy. Data from these experiments might provide useful notions to understand the pathological role of leptin in eating disorders associated with lipodystrophy and action mechanism of leptin on appetite regulation.

Materials and Methods

Subjects

Ten patients with lipodystrophy and 10 healthy subjects participated in the study. Among the 10 patients, six had congenital generalized lipodystrophy (CGL), two had acquired generalized lipodystrophy and the remaining two had Dunnigan-type partial lipodystrophy. Five of the six CGL patients were homozygous or compound heterozygous for mutations in the *seipin* gene (2). The etiology of the remaining CGL patient was unknown. One of the two patients with Dunnigan-type partial lipodystrophy was heterozygous for a mutation in the *LMNA* gene, whereas the other patient had an unknown etiology. For controls, age- and sex-matched healthy subjects with normal weight [body mass index (BMI) between 18.5 and 25.0 kg/m^2] were recruited. None of the control subjects had a past or present history of psychiatric, neurological, endocrine, metabolic, gastrointestinal, or eating disorders, and none was taking medications at the time of study. For both patients and controls, individuals with contraindications for magnetic resonance imaging scanning including claustrophobia and the presence of a cardiac pacemaker or other metallic fragments in the body were excluded. All the subjects had been stable at their body weight for at least 3 months before recruitment. Characteristics of all the subjects are summarized in Supplemental Table 1, published on The Endocrine Society's Journals Online web site at http://jcem.endojournals.org. All the subjects were right-hand dominant according to the Edinburgh Handedness Inventory (22). The means of BMI and basal plasma leptin concentrations in patients were apparently lower than those in controls. All the patients had received leptin-replacement therapy as described below for more than 2 months. For patients, the entire study was conducted during their hospitalization period at Kyoto University Hospital. Study protocols were approved by the Ethical Committee of Kyoto University Graduate School of Medicine. After detailed explanation of the study design and any potential risks, written informed consent was obtained from all subjects before study initiation.

Leptin- replacement therapy

Recombinant methionyl human leptin (meterleptin) was provided by Amylin Pharmaceuticals, Inc. (San Diego, CA). Meterleptin was administered sc once a day at the physiological replacement dose on the basis of information provided by Amylin (1).

Study design

All the fMRI scans were performed at Kyoto University Hospital between 1300 and 1400 h under fasting and postprandial conditions on separate days (Supplemental Fig. 1A). For the fasting condition, subjects were prohibited from eating for 18 h from the night before the examination. For the postprandial condition, subjects ate a meal 1 h before the examination. In addition, fMRI scans were performed for patients with and without leptin treatment (leptin-on and leptin-off, respectively) under both fasting and postprandial conditions. For the leptin-off condition, leptin-replacement therapy was discontinued for more than 4 d. All the subjects were given practice trials outside the scanner and were familiarized with scanning procedures and safety regulations.

fMRI procedures

Blood oxygen level-dependent (BOLD) response to stimuli was measured by fMRI on a 3-Tesla Trio MRI scanner (Siemens, Erlangen, Germany). Whole-brain images were acquired in axial

orientation using the following parameters: repetition time, 3000 msec; echo time, 30 msec; flip angle, 90°; voxel size, 3 × 3 × 3 mm; field of view, 192 × 192 mm; matrix size, 64 × 64; and number of slices, 48. The experiment was conducted in three separate sessions of 18 min, 42 sec each. In each session, 45 food and 30 nonfood pictures were presented randomly in an event-related design (Supplemental Fig. 1B). Food pictures were chosen to suit each subject's taste based on preliminary hearing investigations and included various kinds of food, such as warm meals, desserts, fruits, and vegetables (Supplemental Fig. 1C). Nonfood pictures contained scenery comprising naturally occurring objects, such as trees, bushes, grass, rocks, water, and flowers (Supplemental Fig. 1B). Each picture was presented for 5 sec, followed by 3 sec for the rating image (Supplemental Fig. 1C). Although subjects were presented with rating image, they were asked to rate how much they liked to eat each food or how much they liked each nonfood picture on a scale of 1 (not so appealing) to 4 (highly appealing) by pressing a button with their dominant hand. Next, a mosaic picture was presented for 7 sec as a resting baseline. All pictures were projected onto a screen in the scanner room using Presentation version 9.6 software (Neurobehavioral Systems, Albany, CA) and viewed through a mirror mounted on the head coil. Subjects were instructed to focus all their attention on the pictures.

Image processing and statistical analysis of fMRI data

The fMRI data were preprocessed and statistically analyzed using SPM2 (Wellcome Department of Cognitive Neuroscience, University College London, London, UK) and MATLAB 6.5 (The Mathworks Inc., Natick, MA). Functional images were realigned to the first image and normalized into the Montreal Neurological Institute coordinate by an echo planar imaging template. Normalized images were then smoothed with a 6-mm full-width-at-half-maximum isotropic Gaussian kernel. The functional data were temporally filtered using an autoregressive model and a high pass filter with a cutoff of 128 sec. Five experimental conditions (food picture, nonfood picture, rating for food picture, rating for nonfood picture, and pressing button) were modeled by a function convolved with a hemodynamic response function in the general linear model, and an activation parameter was estimated at each voxel for each stimulus type. Significant signal changes were identified with a voxel-by-voxel analysis on the basis of a comparison of the mean signal amplitude during the periods of stimulation and those of resting baselines, as determined by t test comparisons. At the first level, a statistical parametric map for comparing brain activation to food greater than nonfood was generated for each subject and each condition. These contrast images were then entered into a second level random effect analysis. In the random effects analysis, one-sample t test resulted in images for within-group analysis. For between-group analysis, two-sample t tests created images for control *vs.* patient comparison, and paired t tests created images for leptin-on *vs.* leptin-off comparison. Finally, we transformed the t statistics into Z-scores and generated a Z-score map image. The Z-score maps were then superimposed onto the magnetic resonance images to allow visual inspection of the composite images. We set the significance threshold at $P < 0.05$, false discovery rate (FDR) corrected, for whole-brain analysis, and $P < 0.005$, uncorrected, for region of interest (ROI) analysis with a spatial extent of 10 contiguous voxels. For ROI analysis, brain regions known to be involved in energy homeostasis and appetite regulation were chosen on the basis of previous comparable fMRI studies (23–29). These regions included the hypothalamus, orbitofrontal cortex, amygdala, hippocampus, insula, nucleus accumbens, caudate, putamen, and globus pallidus. ROI were defined using the Wake Forest University Pickatlas (30) and the AAL Talairach Daemon atlas (Research Imaging Center, University of Texas Health Science Center, San Antonio, TX) (31). Regions that were unavailable in these libraries (*e.g.* nucleus accumbens) were drawn within the Wake Forest University Pickatlas using three-dimensional spheres centered at a voxel location determined based on a relevant fMRI study (23).

Measurement of subjective feelings

The participants were asked to provide subjective hunger ratings on a 100-mm visual analog scale (VAS) immediately before every scanning to assess their hunger feelings (32, 33). Higher scores indicated stronger hunger. In addition, appetite was also measured using the mean value of the rating scale for 135 food pictures while viewing them in the scanner. Higher values indicated stronger desire to eat the food in each picture.

Biochemical analyses

Blood samples were obtained in the fasting state. Plasma glucose concentrations were determined by a glucose oxidase method (Arkrey Marketing Inc., Tokyo, Japan), and plasma insulin concentrations were determined by use of an enzyme immunoassay method (TOSOH, Corp., Tokyo, Japan). Plasma leptin concentrations were determined by a competitive RIA method (Millipore Inc., Billerica, MA).

Statistical analysis

Differences between patients and controls in age, BMI, plasma leptin concentration, plasma glucose, and plasma insulin were determined using unpaired t tests. Differences between biochemical values under leptin-on and leptin-off conditions were determined by paired two-tailed t tests. Differences between patients and controls regarding VAS hunger scores and rating scores for food pictures were calculated using repeated measure ANOVA. $P < 0.05$ was considered statistically significant.

Results

Comparison of neural response to food-specific stimuli between healthy controls and patients with lipodystrophy

A within-group analysis of controls and patients for the contrast of food greater than nonfood revealed no significant activation in whole brain analysis at a significance level of $P < 0.05$ (FDR corrected). With a within-group ROI analysis for the contrast food greater than nonfood in healthy controls, significant activation was detected in the bilateral orbitofrontal cortex, amygdala, insula, caudate, putamen, and globus pallidus under the fasting conditions (Fig. 1A). However, significant activation was detected only in the bilateral orbitofrontal cortex and left insula under the postprandial conditions (Fig. 1B). On the other

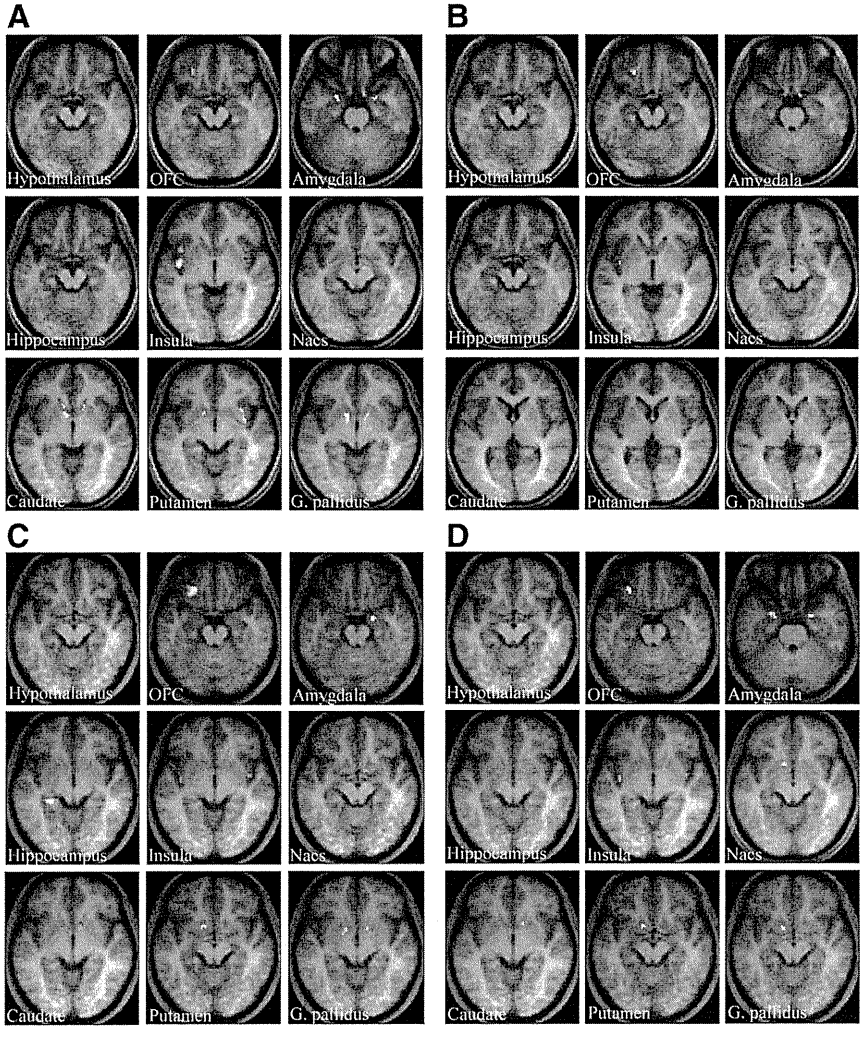

FIG. 1. Neural response to food-specific stimuli in healthy controls and leptin-off patients. Food-specific activations in ROI in the brains of controls (A and B) and patients (C and D) under fasting (A and C) and postprandial (B and D) conditions. Activation is overlaid onto the group average T1-weighted anatomical axial images (*right* is right side of the brain). The *brighter yellow color* represents the higher Z-score. ROI areas are the hypothalamus, orbitofrontal cortex (OFC), amygdala, hippocampus, insula, nucleus accumbens (Nacs), caudate, putamen, and globus pallidus (G. pallidus).

hand, in leptin-off patients, significant activation was detected in the left orbitofrontal cortex, right amygdala, left hippocampus, bilateral insula, bilateral caudate, left putamen, and bilateral globus pallidus under the fasting conditions (Fig. 1C). Significant activation was also detected in most of these areas under the postprandial conditions (Fig. 1D). Coordinates and maximum Z-scores in ROI areas under fasting and postprandial conditions in controls and patients are shown in Supplemental Table 2.

Next, we directly compared the contrast food greater than nonfood between controls and patients by a between-group ROI analysis (Table 1). Under the fasting conditions, a significant difference in activity was detected between controls and patients only in the left insula and left caudate. Activity was down-regulated in the left insula and up-regulated in the left caudate in patients compared with controls. On the other hand, under the postprandial conditions, a significant difference in activity was detected in many areas, including the right orbitofrontal cortex, right amygdala, left insula, left nucleus accumbens, bilateral caudate, left putamen, and left globus pallidus between controls and patients. Activity was up-regulated in all these areas except the right orbitofrontal cortex in patients.

These results indicate that the suppression of neuronal response to food-specific stimuli after a meal is attenuated in patients with lipodystrophy compared with healthy subjects.

Comparison of subjective feelings of appetite between healthy controls and patients with lipodystrophy

Subjective feelings of appetite were evaluated in healthy controls and leptin-off patients. Mean values of the self-reported hunger score on a 100-mm VAS were not significantly different between controls and patients under the fasting conditions (controls: 79.90 ± 4.11; patients: 87.50 ± 4.55) (Fig. 2A). In contrast, under the postprandial conditions, the score was significantly higher in patients than in controls (controls: 17.00 ± 3.09; patients: 53.0 ± 6.76). Consistent with the VAS results, mean values of rating scores for the 135 food pictures were also not different between controls and patients under the fasting conditions (controls: 3.11 ± 0.13; patients: 3.21 ± 0.20), but they tended to be higher in patients than in controls under the postprandial conditions (controls: 2.20 ± 0.24; patients: 2.78 ± 0.23) (Fig. 2B).

These results indicate that the formation of a satiety feeling after a meal is attenuated in patients with lipodystrophy compared with healthy subjects.

Effects of the leptin-replacement therapy on neural response to food-specific stimuli in patients with lipodystrophy

A within-group analysis of leptin-on patients for the contrast food greater than nonfood revealed no significant activation in whole brain analysis at a significance level of $P < 0.05$ (FDR corrected). With a within-group ROI anal-

TABLE 1. Between-group (controls *vs.* leptin-off patients) comparison of brain activations for the contrast food greater than nonfood

		Fasting				Postprandial			
		Coordinate				Coordinate			
Contrast	ROI area	x	y	z	Z-score	x	y	z	Z-score
Controls greater than patients (leptin-off)	Hypothalamus								
	Orbitofrontal cortex					36	44	−12	3.36
	Amygdala								
	Hippocampus								
	Insula	−42	−6	0	3.35				
	Nucleus accumbens								
	Caudate								
	Putamen								
	Globus pallidus								
Patients (leptin-off) greater than controls	Hypothalamus								
	Orbitofrontal cortex								
	Amygdala					22	−4	−22	2.92
	Hippocampus								
	Insula					−46	−12	12	3.10
	Nucleus accumbens					−8	10	−6	3.12
	Caudate					14	2	14	3.21
		−6	10	14	3.46	−8	8	−6	3.50
	Putamen					−10	8	−6	3.48
	Globus pallidus					−10	8	−4	3.41

Coordinate indicates the highest activity voxel of the cluster by Montreal Neurological Institute systems. Negative x-axis coordinates indicate left hemisphere. Z-score represents level of significance.

ysis for the contrast food greater than nonfood under the fasting conditions, significant activation was detected in many brain areas, such as the bilateral orbitofrontal cortex, bilateral amygdala, bilateral hippocampus, bilateral insula, right caudate, right putamen, and bilateral globus pallidus, in leptin-on patients (Fig. 3A). In contrast, neural activity under the postprandial conditions was effectively reduced and significant activation was detected only in the bilateral orbitofrontal cortex and left insula in leptin-on patients (Fig. 3B). Coordinates and maximum Z-scores in ROI areas under the fasting and postprandial conditions in leptin-on patients are shown in Supplemental Table 3.

Next, we directly compared the contrast food greater than nonfood between leptin-on and leptin-off patients by a between-group ROI analysis (Table 2). Under the fasting conditions, a significant difference in neural activity was detected between leptin-on and leptin-off patients only in the left caudate, in which the activity was down-regulated by leptin-replacement therapy in the patients. In contrast, a significant difference in activity was detected in many areas, including the right orbitofrontal cortex, left amygdala, left hippocampus, left insula, bilateral caudate, and left putamen, under the postprandial conditions. The activity was down-regulated in all these areas except the right orbitofrontal cortex by leptin-replacement therapy.

These results indicate that leptin-replacement therapy enhances the suppression of neural response to food-specific stimuli after meal in patients with lipodystrophy.

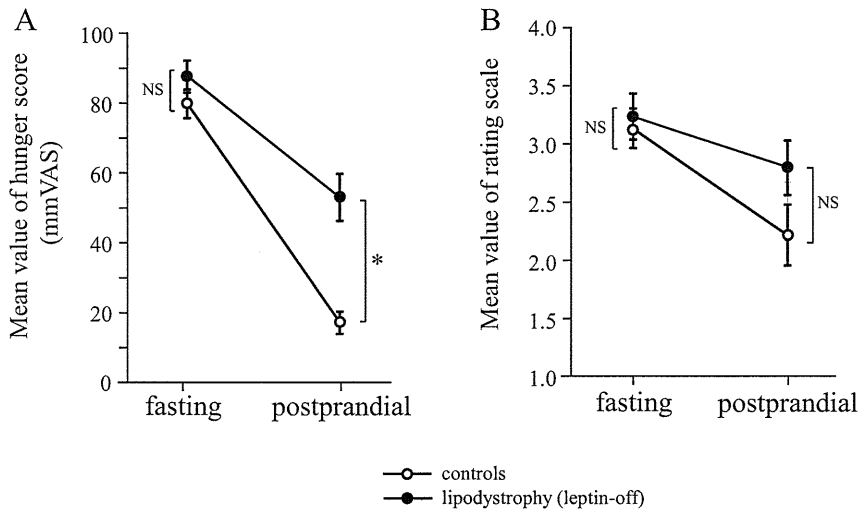

FIG. 2. Subjective feelings of appetite under fasting and postprandial conditions in healthy controls and leptin-off patients. A, Hunger scores on the 100-mm VAS before fMRI scan. B, Mean value of rating scores for food pictures during the fMRI scan. Data are means ± SEM (n = 10 in each group). *, $P < 0.01$ (repeated measure ANOVA).

Effects of the leptin-replacement therapy on subjective feelings of appetite in patients with lipodystophy

We compared subjective feelings of appetite between leptin-on and leptin-off

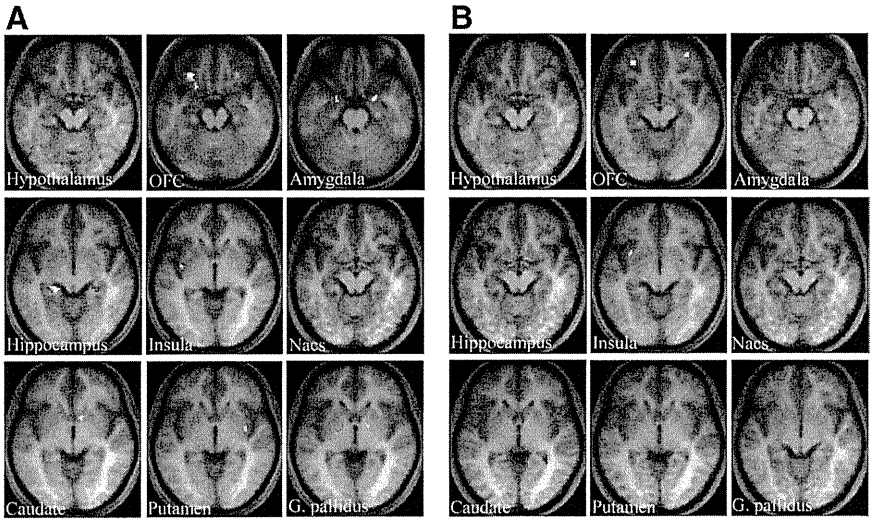

FIG. 3. Neural response to food-specific stimuli in leptin-on patients. Food-specific activations in ROI in the brain under fasting (A) and postprandial (B) conditions. Activation is overlaid onto the group average T1-weighted anatomical axial images (*right* is right side of the brain). The *brighter yellow color* represents the higher Z-score. ROI areas are the same as described in Fig. 1.

patients. Although plasma leptin levels were significantly higher in leptin-on than in leptin-off patients, plasma glucose and insulin levels were not affected by the discontinuation of leptin-replacement therapy for approximately 4 d (Supplemental Table 4). Mean values of self-reported hunger score on a 100-mm VAS were not significantly different between leptin-on and leptin-off patients under the fasting conditions (leptin-on: 83.10 ± 4.40; leptin-off: 87.50 ± 4.55) (Fig. 4A). In contrast, the score was significantly higher in leptin-off than in leptin-on patients (leptin-on: 27.70 ± 5.39; leptin-off: 53.0 ± 6.76) under the postprandial conditions. Consistent with the VAS results, mean values of rating scores for the 135 food pictures were also not different between leptin-on and leptin-off patients under the fasting conditions (leptin-on: 3.17 ± 0.17; leptin-off: 3.21 ± 0.20), but they tended to be higher in the leptin-off than in the leptin-on patients under the postprandial conditions (leptin-on: 2.40 ± 0.26; leptin-off: 2.78 ± 0.23) (Fig. 4B).

These results indicate that leptin-replacement therapy enhances the formation of satiety after meal in patients with lipodystrophy. These results were consistent with the results of fMRI analysis.

Discussion

This is the first report that demonstrates the difference in food-related neural activity between patients with lipodystrophy and healthy controls. A significant difference in food-related neural activity between patients and controls was detected in many brain areas under the postprandial

TABLE 2. Between-group (leptin-on *vs.* leptin-off patients) comparison of brain activations for the contrast food greater than nonfood

		Fasting				Postprandial			
		Coordinate				Coordinate			
Contrast	ROI area	x	y	z	Z-score	x	y	z	Z-score
Leptin-on greater than leptin-off	Hypothalamus								
	Orbitofrontal cortex					32	48	−10	2.98
	Amygdala								
	Hippocampus								
	Insula								
	Nucleus accumbens								
	Caudate								
	Putamen								
	Globus pallidus								
Leptin-off greater than leptin-on	Hypothalamus								
	Orbitofrontal cortex								
	Amygdala					−22	0	−20	2.98
	Hippocampus					−18	−8	−16	3.19
	Insula					−42	−16	10	4.26
	Nucleus accumbens								
	Caudate					6	8	−8	3.46
		−4	6	0	3.02	−4	6	−8	3.34
	Putamen					−8	8	−8	2.90
	Globus pallidus								

Coordinate indicates the highest activity voxel of the cluster by Montreal Neurological Institute systems. Negative x-axis coordinates indicate left hemisphere. Z-score represents level of significance.